Synovium and Capsule

8

Nicolae Bolog, Gustav Andreisek, and Erika Ulbrich

8.1 Anatomy and Normal MRI Appearance

8.1.1 Capsule and Synovial Compartments

The articular capsule of the knee consists of a thick outer layer, the fibrous capsule, and a thinner inner layer, the synovial membrane (synovium).

The synovium is a mesenchymal tissue composed of two to three layers of specialized cells (synoviocytes) and a supporting connective tissue that includes a well-developed vascular network and relatively abundant adipose tissue [1]. This hypervascular membrane is responsible for the secretion of the synovial fluid, which lubricates and nourishes the joint [2]. The synoviocytes also have a role in removing intra-articular particles including cartilaginous debris [2].

The knee joint can be seen as common joint space that is subdivided by synovial membranes into several interconnected compartments. Anteriorly, at the central femoropatellar compartment, the synovial membrane attaches to the patellar borders and extends circumferentially beneath vastus lateralis and vastus medialis muscles to the anterior femoral shaft. It covers also the anterior aspects of the cruciate ligaments. The medial and lateral femorotibial compartments of the synovial membrane are represented by the lateral and medial extensions of the central portion [2]. These compartments are separated by the infrapatellar synovial fold anteriorly and by a reflection of the synovium that extends from the sides of the posterior cruciate ligament onto the fibrous capsule, posteriorly [2]. The anterior and posterior cruciate ligaments, menisci, and the infrapatellar fat pad are located "extrasynovially" which means that they are located outside the abovementioned synovial compartments.

8.1.2 Synovial Bursae and Synovial Recesses

Synovial bursae or synovial recesses are extensions of the synovial membrane between different anatomical structures, and their role is to reduce the friction during the motion of these structures. The knee bursae are numerous and, in the absence of pathological changes, rarely apparent on MR imaging [3]. The knowledge of the locations of synovial bursae is important since in pathological conditions, they may become apparent and a cause for misdiagnosis or diagnostic uncertainty [2]. The classification of the bursae is made on their anatomic location (Table 8.1). Readers of MR images should look for anterior and posterior bursae on sagittal planes and for medial and lateral bursae on axial planes. However, they should have in mind that normal bursae are generally not visible on MR imaging.

N.V. Bolog et al., *MRI of the Knee: A Guide to Evaluation and Reporting*,
DOI 10.1007/978-3-319-08165-6_8, © Springer International Publishing Switzerland 2015

Table 8.1 Anatomy and pathology of synovial bursae and recesses around the knee [2, 3, 5–10]

Compartment	Bursa/recess	Anatomy
Anterior	Suprapatellar bursa (Fig. 8.2)	Located between the quadriceps tendon and femur
	Prepatellar bursa (Fig. 8.3)	Superficially located between the patella and subcutaneous tissue
	Superficial infrapatellar or pretibial bursa	Superficially located between the tibial tubercle and subcutaneous tissue
	Deep infrapatellar bursa (Fig. 8.4)	Located posterior to the distal part of the patellar tendon between the tendon and anterior tibia
	Suprahoffatic recess (Fig. 8.5)	Located close to the inferior border of the patella
	Infrahoffatic recess (Fig. 8.5)	Located anterior to the inferior portion of the infrapatellar plica (also called ligamentum mucosum)
	Central synovial recess (Fig. 8.6)	Located anterior to the anterior cruciate ligament
Posterior	Medial posterior femoral recess or medial gastrocnemius bursa (Fig. 8.7)	Located between the posterior horn of the medial meniscus and the knee capsule and the medial head of the gastrocnemius muscle; may communicate with the articular cavity
	Lateral posterior femoral recess or lateral gastrocnemius bursa (Fig. 8.7)	Located between the posterior horn of the lateral meniscus and the knee capsule and lateral head of the gastrocnemius muscle; may communicate with the articular cavity
	Gastrocnemius-semimembranosus bursa (Fig. 8.8)	Double-bursa located between the semimembranosus and the medial head of the gastrocnemius muscle
	Subpopliteus bursa (Fig. 8.9)	Located between the posterior horn of the lateral meniscus and the popliteus tendon; communicates with the superior tibiofibular joint in 10 % of adults
	Posterior capsular recess (Fig. 8.10)	Located in the midline behind the posterior cruciate ligament; is an extension of the medial femorotibial compartment
Lateral	Iliotibial bursa	Located between the distal portion of the iliotibial band and the adjacent tibia
	Lateral collateral ligament-biceps femoris bursa (Fig. 8.11)	Located at the fibular insertion, the lateral collateral ligament and the biceps tendon form a conjoined tendon. Between the two structures, the lateral collateral ligament-biceps femoris bursa is constantly described
	Parameniscal recesses (Fig. 8.12)	Located superior and inferior to the level of the lateral meniscus in contact with the lateral femoral and tibial condyle
Medial	Medial collateral bursa	Located between the superficial and deep layer of medial collateral ligament
	Pes anserinus bursa	Located between the pes anserinus (tendons of sartorius, gracilis, and semitendinosus muscles) and the medial collateral ligament; does not typically communicate with the joint
	Medial collateral ligament-semimembranosus bursa	Located between the semimembranosus tendon and the medial collateral ligament

8.1.3 Synovial Plicae

Synovial plicae are normal anatomical structures representing embryologic remnants of the synovial membrane and are defined as thin, vascularized synovial folds without a known function [2, 4]. The plicae are usually asymptomatic, and they can be found at MR imaging within the knee joints as low-signal-intensity thin bands (Fig. 8.1). The most encountered plicae of the knee are the suprapatellar plica, the infrapatellar plica, the lateral patellar plica, and the mediopatellar plica (Table 8.2).

8.2 MRI Pathological Findings

8.2.1 Joint Effusions

Synovial Fluid

The synovial fluid is a viscid fluid secreted by the synovium. The knee synovial fluid is commonly depicted on MR imaging, but a definitive criterion that enables to define the quantity of the effusion as normal or pathological has not been clearly established. Clinically, knee effusions of less than 6–8 mL cannot be appreciated. However, on MR imaging, a volume of 1 mL of effusion may be visible adjacent to the femoral condyles [13]. Some authors demonstrated that a volume of 4 mL of fluid is depicted on plain radiography and, on midline sagittal MR images, leads to an anteroposterior diameter of the midline suprapatellar recess of 4 mm [13, 14]. This volume of

Fig. 8.1 Suprapatellar plica in a 28 year old female. Sagittal T2-weighted fat-suppressed image shows the synovial plica as a low-signal-intensity thin band (*arrow*)

Table 8.2 Synovial plicae of the knee [4, 11, 12]

	Anatomy	MR imaging appearance
Suprapatellar plica (Fig. 8.13)	Located between the suprapatellar bursa and the knee joint cavity; runs from the posterior aspect of quadriceps tendon, above the patella upward to the anterior aspect of the femur	Low-signal-intensity linear band posterior to the patella
Infrapatellar plica or ligamentum mucosum (Fig. 8.14)	The most commonly plica in the knee; runs from the femoral origin anterior to the intercondylar notch downward to the inferior pole of the patella	Low-signal-intensity band of various dimensions anterior and parallel to the anterior cruciate ligament, often within the infrapatellar fat pad
Mediopatellar plica (Fig. 8.15)	Runs from the medial capsule of the knee obliquely downward to the synovium of the infrapatellar fat pad	Low-signal-intensity linear band that may be connected to the suprapatellar plica; can extend between the medial facet of the patella and medial face of the trochlea
Lateral patellar plica (Fig. 8.16)	The least common plica of the knee; runs from the popliteus hiatus and attaches to the infrapatellar fat pad	Low-signal-intensity linear longitudinal band 1–2 cm lateral to the patella

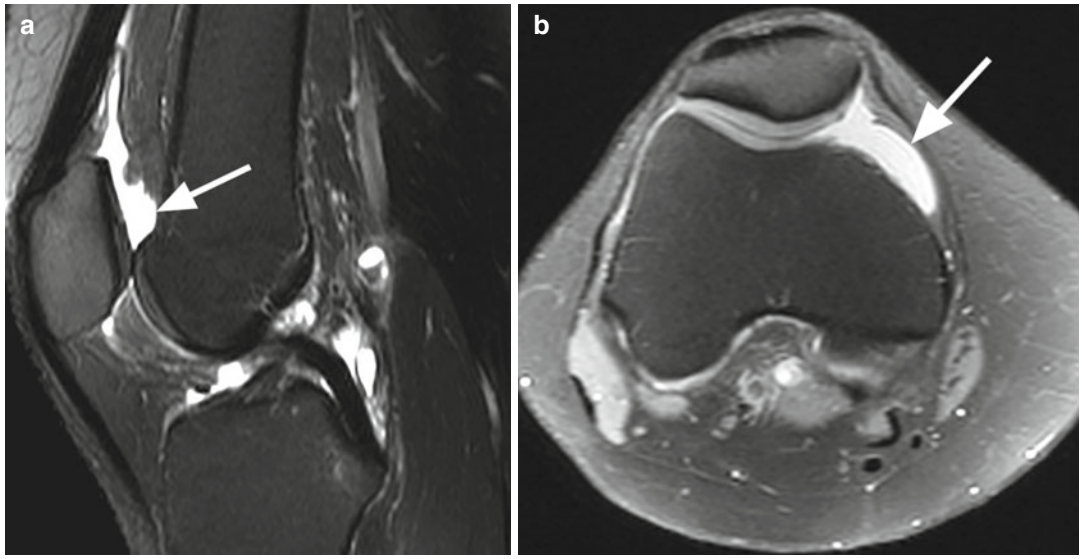

Fig. 8.2 Suprapatellar bursa in a 40 year old female. Sagittal T2-weighted fat-suppressed image (**a**) and axial proton-density (PD) fat-suppressed image (**b**) show the fluid in the suprapatellar bursa (*arrow*)

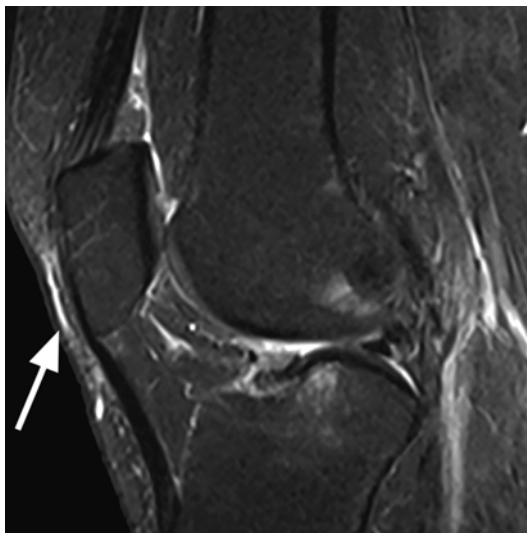

Fig. 8.3 Prepatellar bursa in a 55 year old male. Sagittal T2-weighted fat-suppressed image shows a small amount of fluid in the prepatellar bursa (*arrow*)

Fig. 8.4 Deep infrapatellar bursa in a 22 year old female. Sagittal T2-weighted fat-suppressed image shows the deep infrapatellar bursa posterior to the distal part of the patellar tendon between the tendon and anterior tibia (*arrow*)

effusion was considered to be clinically important [15]. With increasing volumes of effusion, the fluid first collects in the suprapatellar bursa and subsequently in the posterior recesses and popliteal tendon sheath [13].

Although the knee effusion may be the only finding on MR imaging, most commonly the synovial fluid is the result of a different underlying pathology (e.g., inflammatory diseases, trauma, degenerative changes, tumors). On MR imaging, the joint fluid appears homogeneously

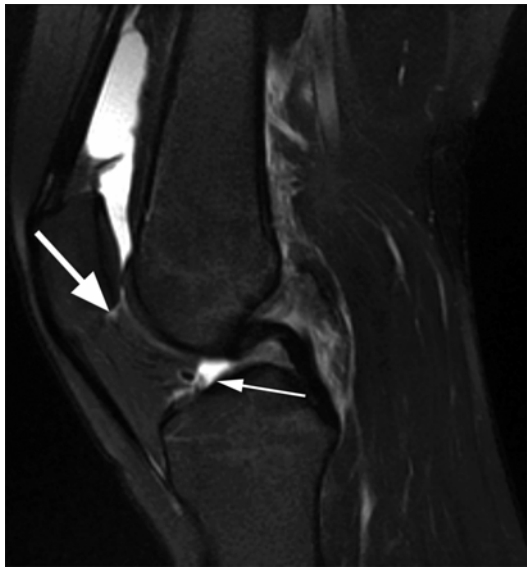

Fig. 8.5 Suprahoffatic and infrahoffatic recesses in a 19 year old female. Sagittal T2-weighted fat-suppressed image shows the suprahoffatic recess (*large arrow*) close to the inferior border of the patella and the infrahoffatic recess (*small arrow*)

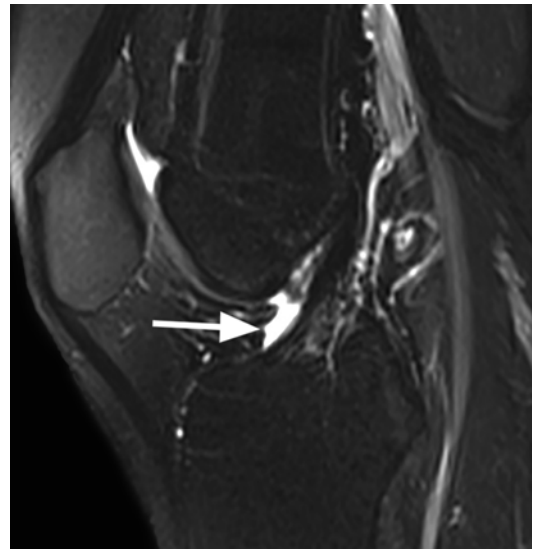

Fig. 8.6 Central synovial recess in a 30 year old female. Sagittal T2-weighted fat-suppressed image shows the recess located anterior to the anterior cruciate ligament (*arrow*)

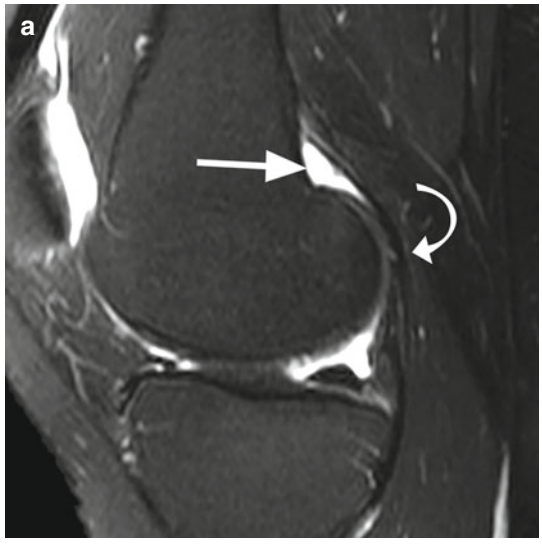

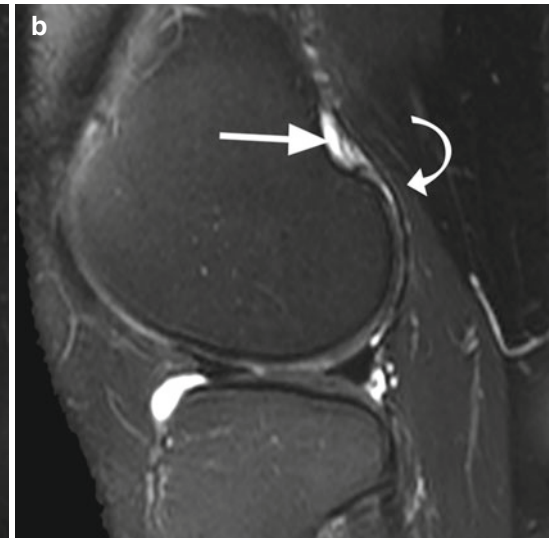

Fig. 8.7 Medial posterior femoral recess (medial gastrocnemius bursa) and lateral posterior femoral recess (lateral gastrocnemius bursa) in a 40 year old female. Sagittal T2-weighted fat-suppressed images through the medial compartment (**a**) and lateral compartment (**b**) show the medial gastrocnemius bursa (*arrow* in **a**) between the knee capsule and the medial head of the gastrocnemius muscle (*curved arrow* in **a**) and the lateral gastrocnemius bursa (*arrow* in **b**) between the knee capsule and the lateral head of the gastrocnemius muscle (*curved arrow* in **b**)

hypointense or of intermediate signal intensity on T1-weighted images and hyperintense on T2-weighted images.

Hemarthrosis and Lipohemarthrosis

Hemarthrosis is the result of the hemorrhage within the joint due to ligamentous injury, bone

fracture, patellar dislocation, or other diseases including pigmented villonodular synovitis, hemophilia, articular tumors, neuroarthropathy, gout, and anticoagulant therapy [12, 16, 17]. The MRI appearance of hemarthrosis depends on the stage of the hemorrhage. In the early stage, the hemorrhage has a double-layer fluid level appearance with a superior layer of blood serum floating on an inferior layer of cellular debris of intermediate signal intensity on T1- and T2-weighted images. Gradient-echo images are especially useful for the identification of blood products due to the "blooming" effect.

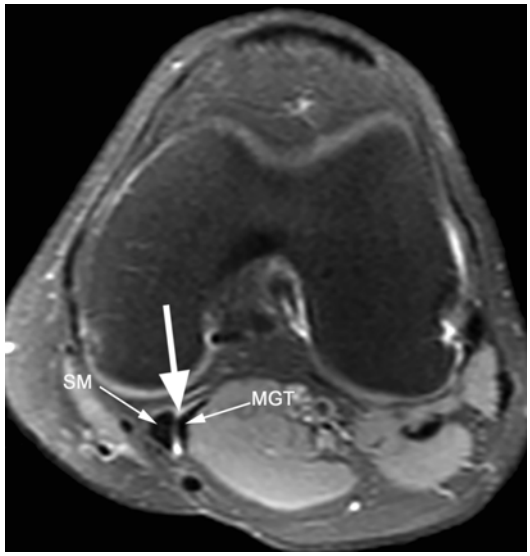

Fig. 8.8 Gastrocnemius-semimembranosus bursa (popliteal cyst or Baker's cyst) in a 36 year old male. Axial proton-density (PD) fat-suppressed image shows a small amount of fluid in the popliteal bursa (*arrow*) which is located between the semimembranosus (*SM*) and the medial head of the gastrocnemius muscle (*MGT*)

Lipohemarthrosis, the presence of blood and fat within the joint, is a very strong indicator for intraarticular fracture. Most commonly, lipohemarthrosis is seen on MR imaging as a three-layer fluid level that appears approximately 3 h after trauma (Fig. 8.17) [18]. The superior layer with fat signal intensity (hyperintense on T1- and T2-weighted images and hypointense on fat-suppressed images) represents the floating fat. The intermediate or the central layer appears as a normal joint fluid and represents the blood serum, and the inferior layer of cellular debris is seen as intermediate signal intensity on T1- and T2-weighted images. In the very early stage, lipohemarthrosis may show a double-layer appearance with entrapment of globules of fat [18].

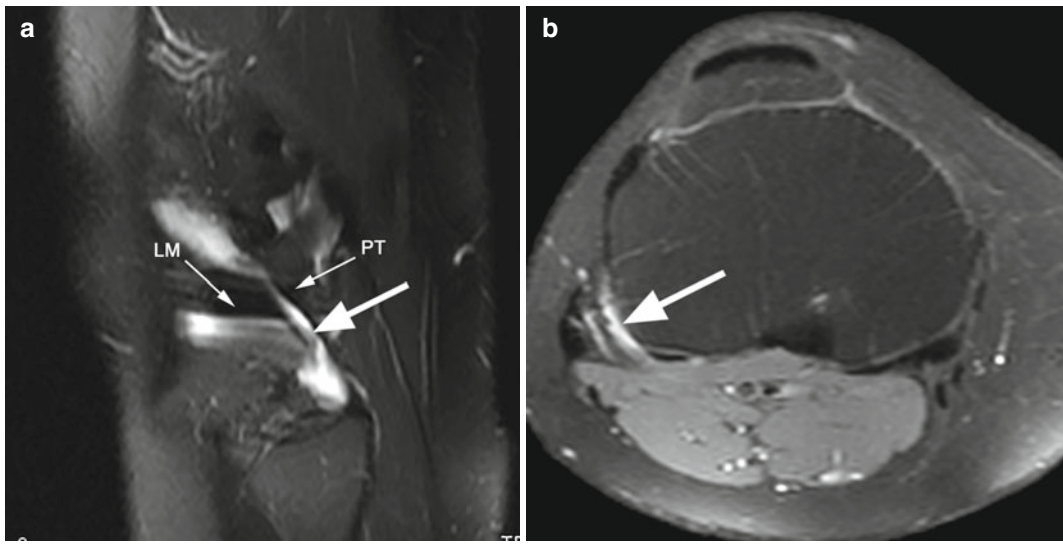

Fig. 8.9 Subpopliteus bursa in a 40 year old female. Sagittal T2-weighted fat-suppressed image (**a**) and axial proton-density (PD) fat-suppressed image (**b**) show the subpopliteal bursa (*large arrow* in **a**, **b**) located between the posterior horn of the lateral meniscus (*LM*) and the popliteus tendon (*PT*)

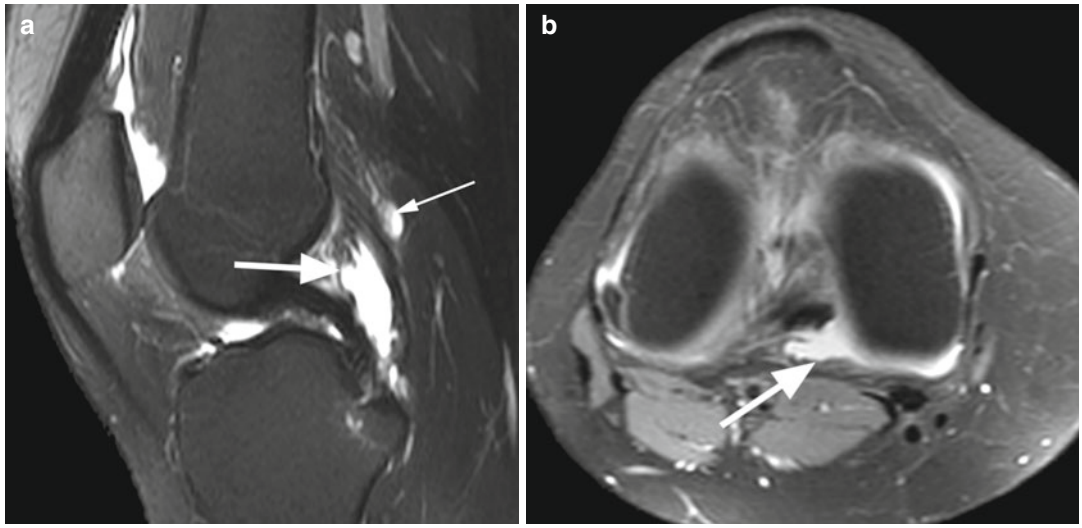

Fig. 8.10 Posterior capsular recess in a 40 year old female. Sagittal T2-weighted fat-suppressed image (**a**) and axial proton-density (PD) fat-suppressed image (**b**) show the posterior capsular recess (*large arrow* in **a**, **b**) located in the midline behind the posterior cruciate ligament. In cases of posterior capsule lesions, the fluid from this recess may be identified posteriorly to the capsule (*small arrow* in **a**)

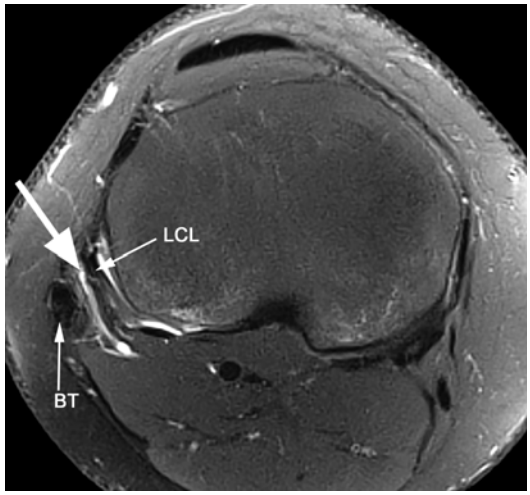

Fig. 8.11 Lateral collateral ligament-biceps femoris bursa in a 25 year old male. Axial proton-density (PD) fat-suppressed image shows a small amount of fluid in the lateral collateral ligament-biceps femoris bursa (*large arrow*) which is located between the lateral collateral ligament (*LCL*) and the biceps femoris tendon (*BT*)

Fig. 8.12 Parameniscal recesses in a 41 year old male. Coronal proton-density (PD) image shows the parameniscal recesses (*arrows*) in contact with the lateral femoral and lateral tibial condyle

8.2.2 Intra-articular Bodies

Intra-articular bodies are best depicted on MR imaging in the presence of joint effusion as they are nicely outlined by the surrounding joint fluid. They appear as filling defects within the fluid (Figs. 8.18, 8.19, 8.20, and 8.21). The best technique to visualize intra-articular bodies is direct MR arthrography where the contrast agent is administered directly into the joint space increasing the amount of the intra-articular joint fluid. However, in the knee, intra-artic-

Fig. 8.13 Suprapatellar plica in a 33 year old male. Sagittal proton-density (PD) image shows the suprapatellar plica within the suprapatellar fat pad (*arrow*). The plica appears thickened indicating a suprapatellar plica syndrome

Fig. 8.14 Infrapatellar plica or ligamentum mucosum in a 43 year old male. Sagittal T2-weighted fat-suppressed image shows the ligamentum as low-signal-intensity thin band (*large arrow*) anterior and parallel to the anterior cruciate ligament. Note the fluid in the central synovial recess (*small arrow*)

ular bodies are often large, and usually there is enough joint fluid present. Thus, MR arthrography in the knee for the detection of intra-articular

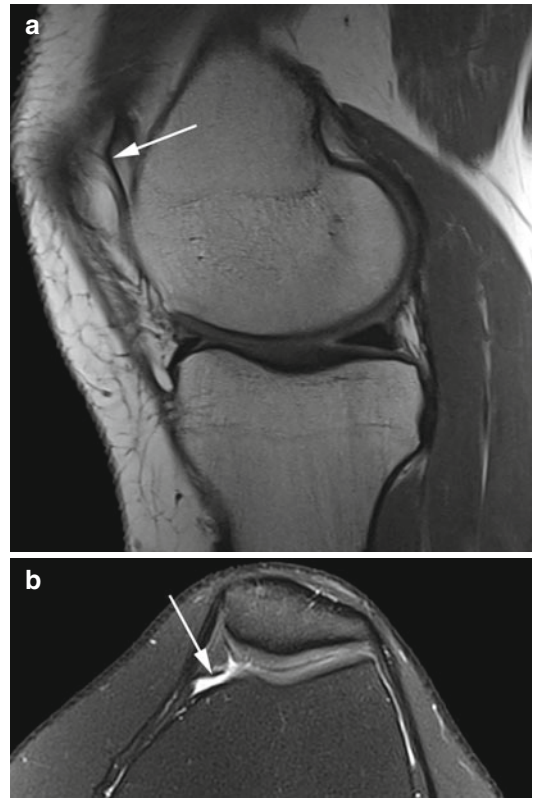

Fig. 8.15 Mediopatellar plica in a 26 year old male. Sagittal proton-density (PD) image (**a**) and axial proton-density (PD) fat-suppressed image (**b**) show a normal mediopatellar plica (*arrow* in **a**, **b**) as a thin low-signal-intensity band in the medial suprapatellar fat pad

bodies is not recommended as a standard procedure, but can be helpful in cases where intra-articular bodies are suspected but cannot be otherwise detected.

Intra-articular bodies may have different etiologies, and the MRI signal appearance depends on the structure and origin of the bodies (Table 8.3). In the knee, intra-articular bodies are usually found beneath the medial collateral ligament, within the intercondylar notch, and in the tendon sheath of the popliteus tendon, or they can migrate into Baker's cysts [12]. It needs to be noted that intra-articular bodies are difficult to detect during arthroscopy, i.e., when they are located in recesses or compartments, which are hardly or even non-accessible by the arthroscope.

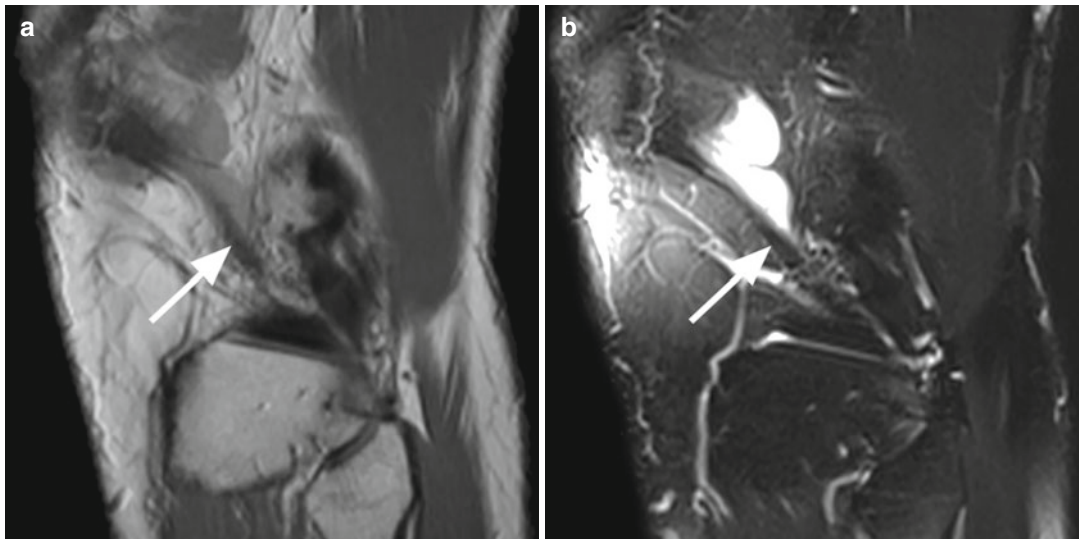

Fig. 8.16 Lateral patellar plica in a 38 year old male. Sagittal proton-density (PD) image (**a**) and sagittal T2-weighted fat-suppressed image (**b**) show the lateral patellar plica (*arrow* in **a**, **b**) extending from the popliteus hiatus to the patella

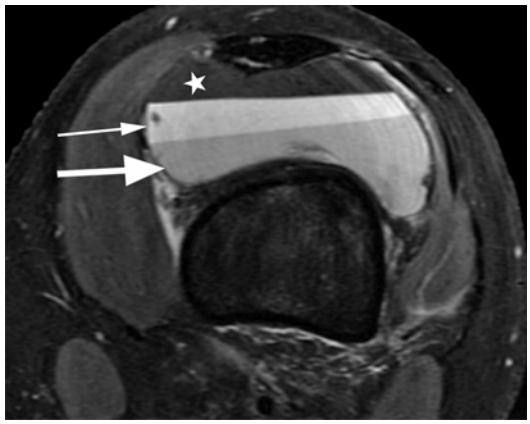

Fig. 8.17 Lipohemarthrosis in a 16 year old female. Axial proton-density (PD) fat-suppressed image shows the superior layer of floating fat which appears hypointense on fat-suppressed sequences (*star*), the intermediate or the central layer which appears as a normal joint fluid and represents the blood serum (*small arrow*), and the inferior layer of cellular debris which is seen as intermediate signal intensity (*large arrow*)

8.2.3 Synovitis

Synovitis, the inflammation of the synovial membrane, can be the result of several disorders including inflammatory arthritis, osteoarthritis, infection, pigmented villonodular synovitis, chronic intra-articular hemorrhage, metabolic diseases, tumors, and trauma. The MR imaging diagnosis of synovitis is based on the evaluation of the synovium thickness and the presence of synovial effusion. The synovial hypertrophy may involve the entire knee synovium or may be focal and is seen on T2-weighted and on gradient-weighted images as hyperintense synovial membrane having a thickness of more than 2–3 mm (Fig. 8.22) [19]. A better appreciation of synovitis is obtained on postcontrast T1-weighted MR images that enable a superior delineation of the hypertrophied synovial membrane from the joint effusion (Fig. 8.23). Due to hyperemia of the inflamed synovium, there is an increased synovial enhancement on postcontrast T1-weighted images that can be also used to differentiate between acute and chronic inflammation.

Signal alterations in Hoffa's fat pad are a finding that can be seen in a multitude of diseases and can be used as a surrogate for knee synovitis [20–22].

Inflammatory Synovitis in Rheumatological Disorders

In rheumatological disorders (rheumatoid arthritis, psoriatic arthritis, and ankylosing spondylitis), the synovium is affected first, followed by involvement of the cartilage and bones. MR imaging

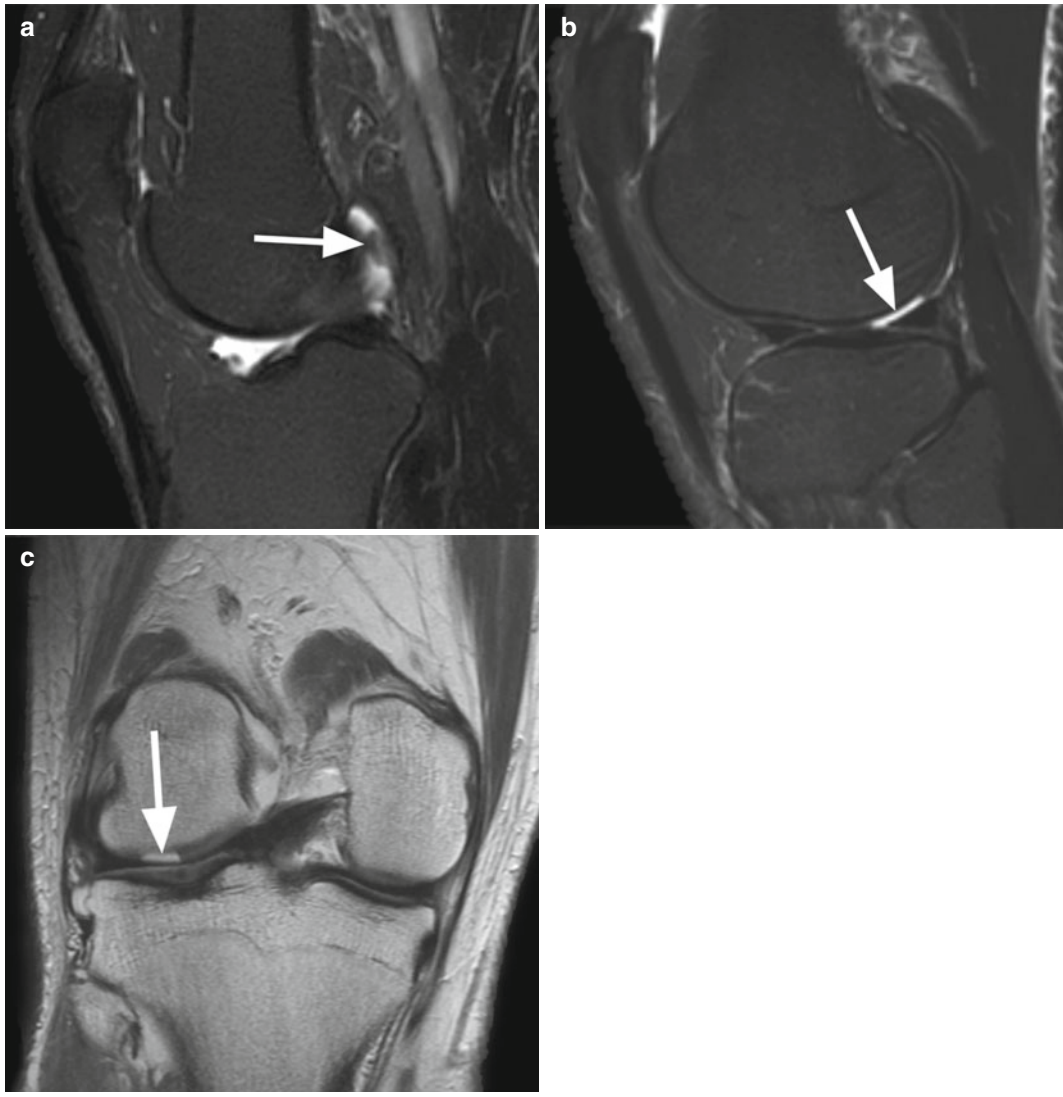

Fig. 8.18 Intra-articular free cartilage fragment in a 43 year old male. Sagittal T2-weighted fat-suppressed image (**a**) shows a small fragment of cartilage surrounded by joint fluid (*arrow*). Sagittal T2-weighted fat-suppressed image (**b**) and coronal proton-density (PD) image (**c**) demonstrate the lateral femoral condyle as the donor site (*arrows* in **b**, **c**)

enables the diagnosis of all intra-articular pathological changes including synovitis and joint effusion, bone marrow edema, and subchondral erosions (Fig. 8.20). There are different MRI techniques used in the evaluation of the synovial proliferation that are used either for qualitative or quantitative evaluation. Synovitis is best identified on T2-weighted images and postcontrast T1-weighted images as uniform or irregular thickening of the synovial membrane. Different quantitative evaluations of synovitis have been described including the synovial volume measurement and the rate of contrast enhancement. Dynamic contrast-enhanced T1-weighted sequences may differentiate between active and chronic phases of the disease with a rapid synovial enhancement (30–60 s) after contrast administration in active or acute phases [23, 24]. Nevertheless, synovial volume or enhancement rate measurements require post-processing work, which is time consuming in clinical practice and thus rarely used [12]. Apart from demonstrating the synovial proliferation,

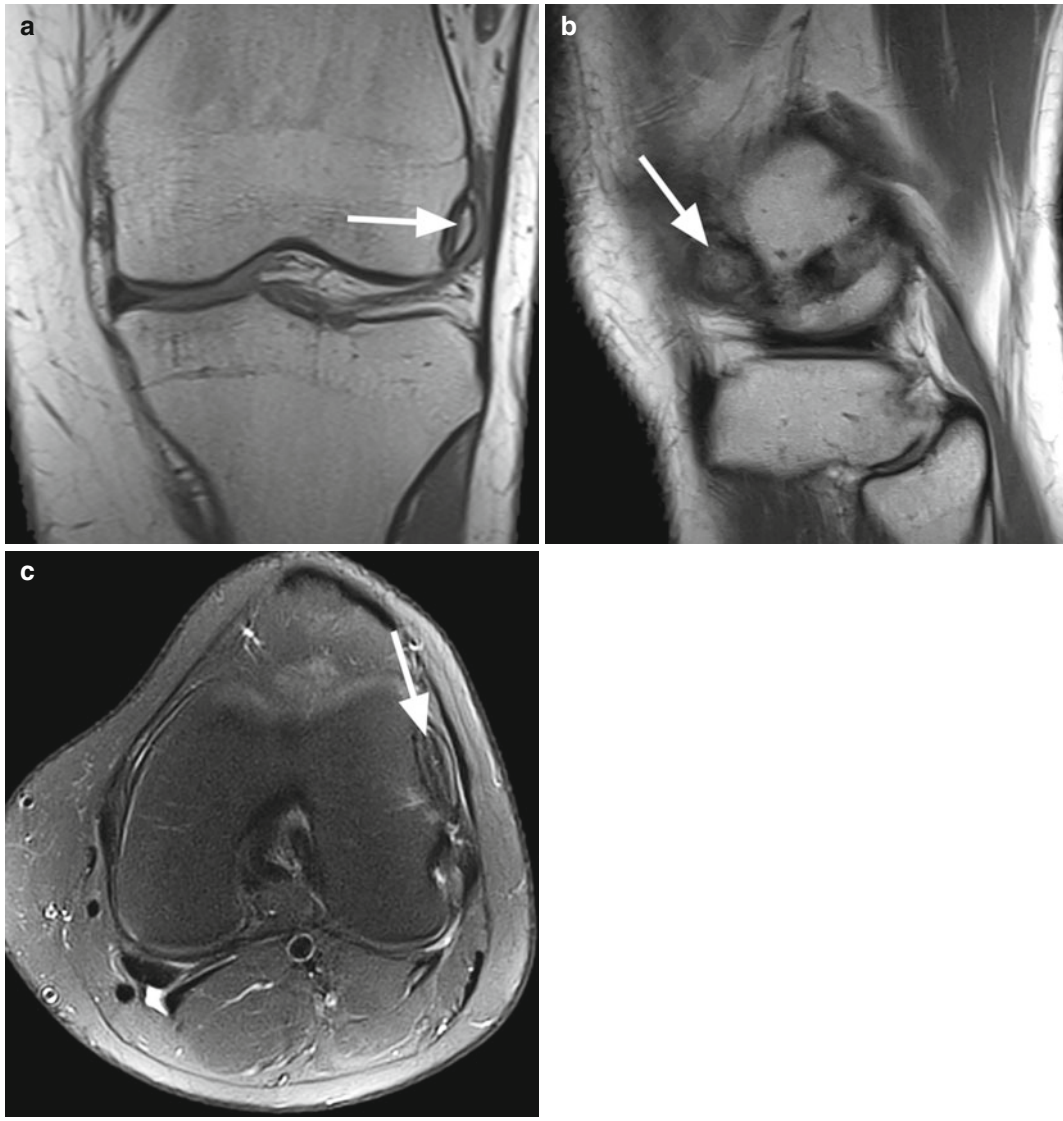

Fig. 8.19 Detached bone fragment in a 21 year old female 3 years after knee injury. Coronal T1-weighted image (**a**), sagittal proton-density (PD) image (**b**), and axial proton-density (PD) fat-suppressed image (**c**) show a bone fragment detached from the lateral femoral condyle (*arrows*). The chronicity of the condition is demonstrated by the synovial reaction around the lesion and the absence of bone marrow edema

MRI demonstrates periarticular inflammation and tendon and ligament inflammation as well as complications such as ruptures of the tendons, presence of "rice-bodies" bursitis, osteonecrosis, and stress fractures [25, 26].

Although rheumatoid arthritis and the seronegative spondyloarthropathies share similar pathological changes, several findings can narrow the differential diagnosis [12]. In rheumatoid arthritis, there are symmetrical abnormalities, and the extent of subchondral erosions and the degree of synovial inflammation are more prominent. However, intra-articular rheumatoid nodules are rarely seen [27]. The rheumatoid nodules are solitary or multiple nodules that appear as inhomogeneous isointense or hypointense lesions on T1-weighted images and inhomogeneous isointense or hyperintense on T2-weighted

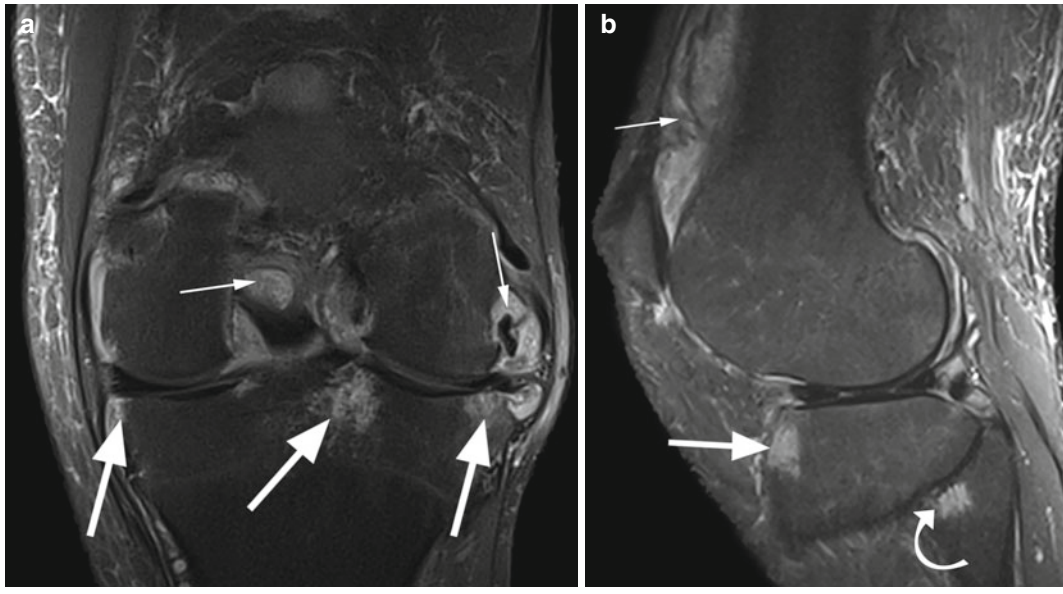

Fig. 8.20 Rheumatoid arthritis in a 45 year old male. Coronal proton-density (PD) fat-suppressed image (**a**) shows small innumerable nodules within the synovial membrane (*small arrows*). Subchondral erosions are seen in the tibial subchondral bone (*large arrows*). Sagittal T2-weighted fat-suppressed image (**b**) also shows subchondral bone marrow edema of the anterior tibial plateau (*large arrow*), synovitis (*small arrow*), and erosion of the fibular head (*curved arrow*)

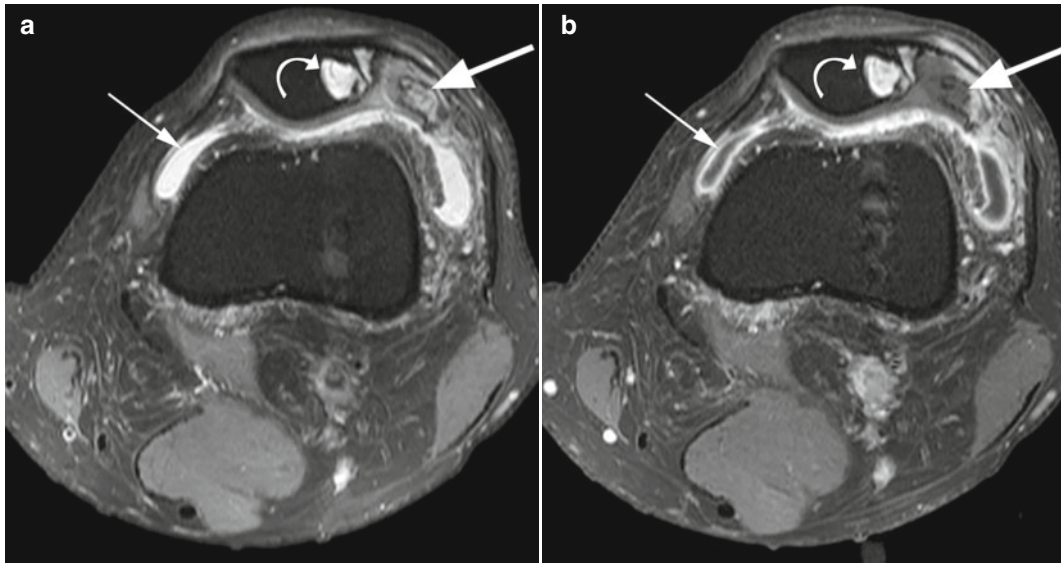

Fig. 8.21 Acute gout in a 55 year old male. Axial proton-density (PD) fat-suppressed image (**a**) and axial T1-weighted fat-suppressed postcontrast image (**b**) show the gout tophus of relatively high signal intensity on a fat-suppressed image (*large arrow* in **a**) but without enhancement after contrast administration (*large arrow* in **b**). Subchondral cysts are seen within the adjacent patella (*curved arrows* in **a**, **b**) resulting from repetitive gout attacks. The synovia is thickened and joint effusion is present (*small arrows* in **a**, **b**)

Table 8.3 Etiology and MRI appearance of intra-articular bodies [12]

Etiology/structure	MRI findings
Cartilage/meniscus (Fig. 8.18)	Similar signal intensity with joint cartilage/meniscus; MR images should be carefully scrutinized for donor site; the size of the body should match the size of the donor site
Bone (Fig. 8.19)	Signal intensity of bone marrow; MR images should be carefully scrutinized for donor site
Osteochondral fragment	Cortical bone of low signal intensity on all MR sequences with attached cartilage of intermediate signal intensity on T1- and T2-weighted; may mirror the defect at the donor site
Inflammatory synovitis (including tuberculosis) (Fig. 8.20)	Intermediate- to low-signal-intensity small innumerable nodules along the synovial membrane (rice bodies)
Gout (Fig. 8.21)	Soft tissue tophi of monosodium urate crystal deposits with inhomogeneous T2-weighted signal intensity; enhances after i.v. contrast administration
Primary synovial osteochondromatosis	Multiple circumscribed nodules of metaplastic hyaline cartilage (range from 2.0 mm to more than 1.0 cm); the signal intensity varies according to the maturity of the nodules and the presence of calcifications within the nodules; may present as conglomerate mass
Pigmented villonodular synovitis	Conglomerate or scattered nodules within the joint; low signal intensity on T1-weighted images and low to high signal intensity on T2-weighted images; "blooming" on gradient-echo images due to iron deposition
Hemophilic arthropathy	Similar appearance with pigmented villonodular synovitis
Metallic foreign bodies	Filling defects with susceptibility artifacts
Intra-articular gas	Low-signal-intensity globular filling defects with "blooming" on gradient-echo images

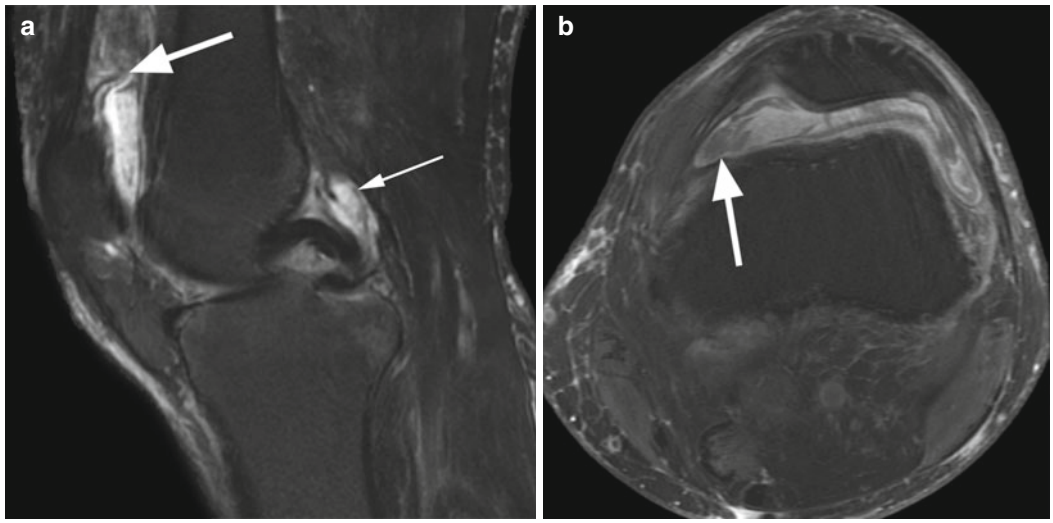

Fig. 8.22 Chronic synovitis in a 65 year old male. Sagittal T2-weighted fat-suppressed image (**a**) and axial proton-density (PD) fat-suppressed image (**b**) show a synovium with a thickness of more than 3 mm but without a clear delineation from the joint fluid (*large arrows* in **a**, **b**). Note the diffuse involvement of the entire synovium including the posterior recess (*small arrow* in **a**)

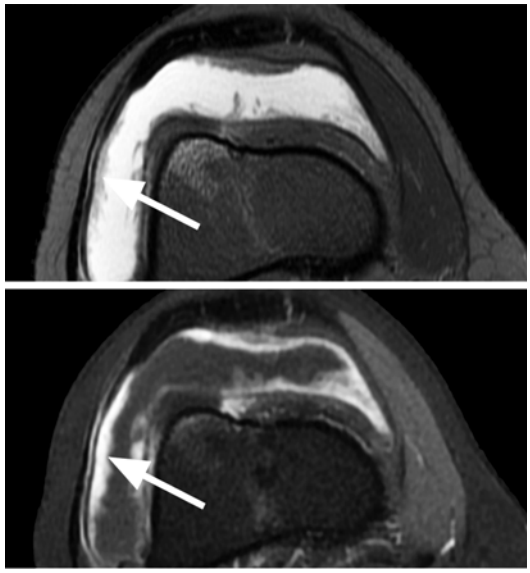

Fig. 8.23 Acute synovitis in a 25 year old female. Axial proton-density (PD) fat-suppressed image (**a**) shows synovial hypertrophy and irregularity (*arrow*). Axial T1-weighted fat-suppressed postcontrast image (**b**) shows an increased enhancement and enables a superior delineation of the hypertrophied synovial membrane (*arrow*) from the joint effusion

images compared with muscles (Fig. 8.24). They may enhance homogeneously or heterogeneous predominantly in the periphery. In ankylosing spondylitis and other seronegative spondyloarthropathies, the knee joint is involved in 30 % of the patients with long-standing disease, and the bone marrow edema has a perientheseal distribution that is not commonly seen in patients with rheumatoid arthritis [12, 28]. The osseous fusion is also more common in seronegative spondyloarthropathies. Overall, however, differential diagnosis remains difficult on MR images, and in the clinical routine, one might not be disappointed when a final diagnosis cannot be made with 100 % confidence.

Synovitis in Osteoarthritis

Synovial proliferation and joint effusion in osteoarthritis is the result of ligament injuries, loose bodies, cartilage deterioration, and meniscal damage (Fig. 8.25) [29, 30]. Synovitis is present even in the early phase of osteoarthritis, and there is evidence that synovial proliferation is not only

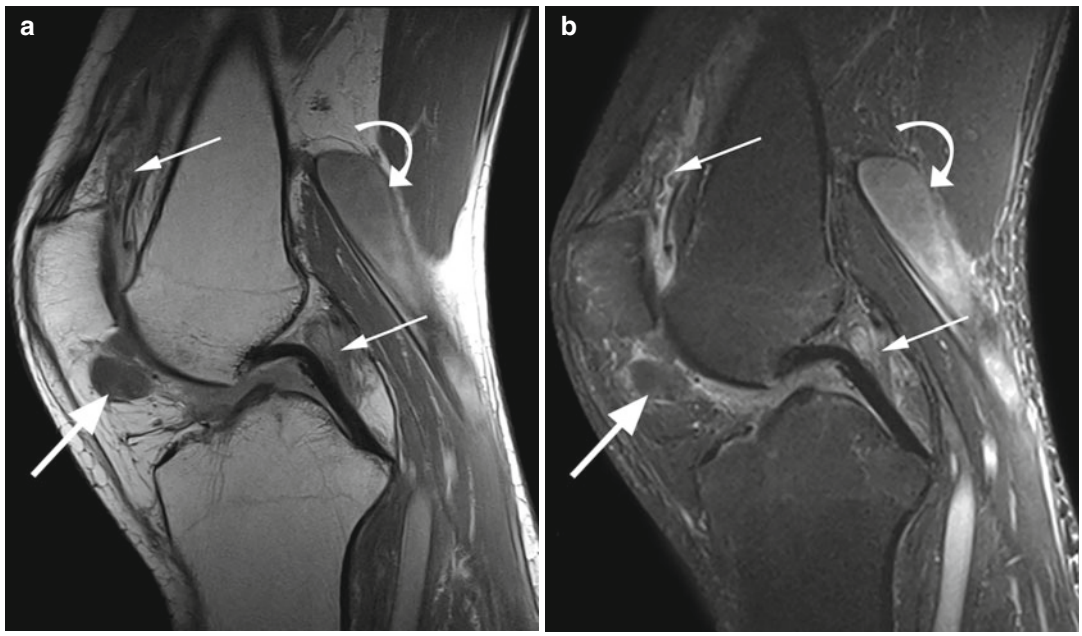

Fig. 8.24 Rheumatoid nodules in a 45 year old male with rheumatoid arthritis. Sagittal proton-density (PD) image (**a**) and sagittal T2-weighted fat-suppressed image (**b**) show two infrapatellar nodules with signal intensity similar to muscles (*large arrows* in **a**, **b**). Note the synovitis in the suprapatellar bursa and central recesses (*small arrows* in **a**, **b**) as well as the inflammation of the Baker's cyst (*curved arrow* in **a**, **b**) which appears with inhomogeneous signal intensity and diffuse pericystic changes

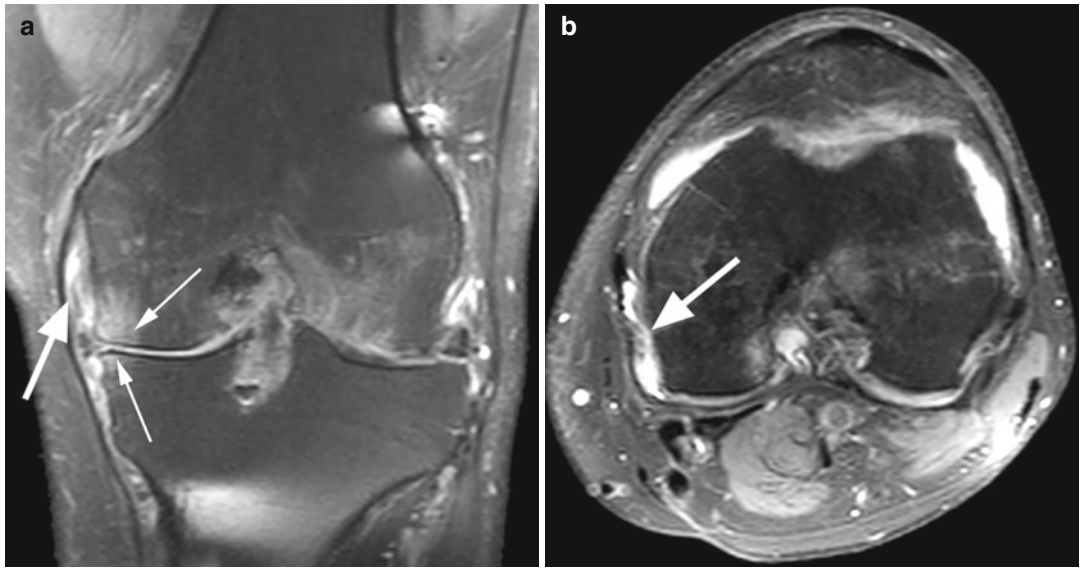

Fig. 8.25 Chronic medial collateral bursitis in a 45 year old male with advanced medial knee osteoarthritis. Coronal proton-density (PD) fat-suppressed image (**a**) and axial proton-density (PD) fat-suppressed image (**b**) show the presence of fluid between the superficial and the deep layers of the medial collateral ligament (MCL) (*large arrows* in **a**, **b**). Note the subchondral edema and the cartilage absence in the medial compartment (*small arrows* in **a**)

a secondary phenomenon but that it also plays a role in progression of cartilage loss [29]. Synovial inflammation is believed to contribute to pain in patients with knee osteoarthritis, and several studies have indeed shown that high-grade synovitis in patients with knee osteoarthritis is statistically associated with pain [29, 31].

Infectious Synovitis

The imaging findings in infectious synovitis are nonspecific, and MRI cannot differentiate septic from nonseptic arthritis. The clinical history is key for differential diagnosis. Early detection of infectious synovitis is crucial in the treatment management and in preventing bone deformities. Thus, if there is clinical suspicion for infection, MR should be performed immediately and any destructive monoarticular process should be regarded as infection until proven otherwise [12]. There are several MRI findings that suggest an infectious etiology. These include synovial thickening, soft tissue edema, and extensive bone marrow edema with enhancement involving both sides of articulation and bone erosions (Fig. 8.26) [32, 33]. Inhomogeneous joint effusion with septa and debris or the presence of synovial or bone abscess is highly correlated with septic arthritis (Fig. 8.26). The evolution and the variation of the imaging findings can help narrowing down the differential diagnosis. In bacterial arthritis, there is a rapid evolution with extensive erosions, whereas in tuberculosis, the evolution is slow and the granulation inflammatory tissue extends in the subchondral bone (pannus) [12].

Hemosiderotic Synovitis

Hemosiderotic synovitis occurs in hemophiliac males because of chronic intra-articular hemorrhage. The knee joint is particularly often involved, and the patients develop osteoarthritis and complain of pain and stiffness of the joint [34, 35]. Due to repetitive hemorrhage, the synovium becomes thickened owing to intrasynovial fibrous scarring [34]. The absorption of hemosiderin by the synovial membrane leads to inflammation and hypertrophy with pannus formation extending throughout the cartilage into the subchondral bone. MR imaging identifies the thickened synovium and hemarthrosis as well as subchondral cysts and erosions (Fig. 8.27). The thickened synovium is best appreciated on post-contrast T1-weighted images. On gradient-echo

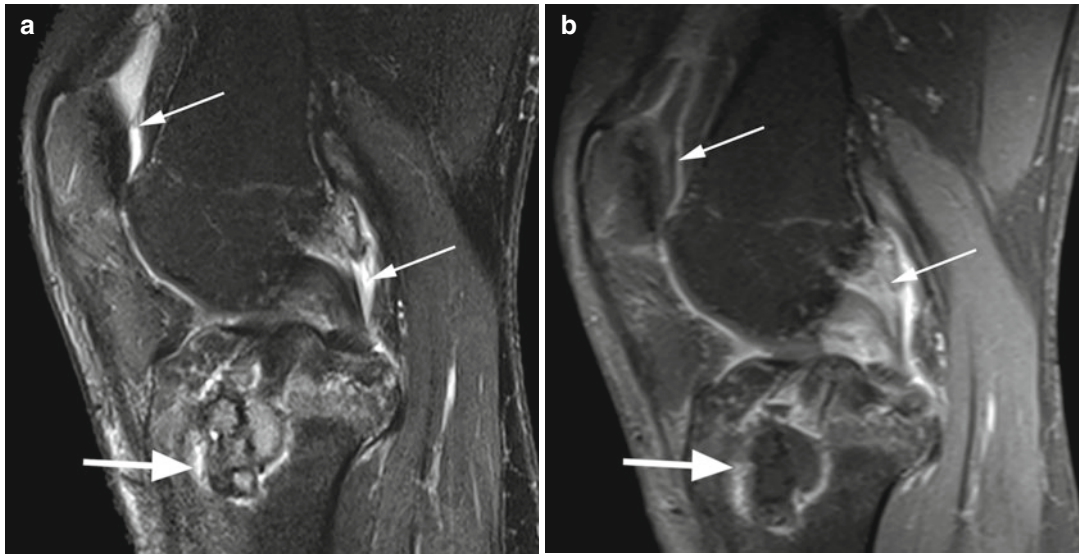

Fig. 8.26 Infectious arthritis in a 32 year old female after anterior cruciate (ACL) reconstruction. Sagittal T2-weighted fat-suppressed image (**a**) and sagittal T1-weighted fat-suppressed postcontrast image (**b**) show an abscess of the tibial plateau (*large arrows* in **a** and **b**). The synovia is thickened and shows increased enhancement of the synovial membrane in the suprapatellar bursa and the pericruciate area (*small arrows* in **a** and **b**)

sequences, blooming artifacts are characteristic for the hemosiderin-laden synovium and helpful for detection in early phases of the disease [36]. Hemosiderotic synovitis can be found also in patients with intrasynovial hemangiomas for which the knee joint is the most frequently involved site [37].

Arthridities and Metabolic Diseases

Gout

Gout is a rheumatological disorder characterized by urate crystal deposition within the joint. The tophi vary from a few millimeters to 5 cm and can be localized in the capsule, the synovium, the articular cartilage, the subchondral bone, and the periarticular soft tissue. In the acute phase, there is thickening of the synovia and effusion, and the tophi are isointense or hypointense to muscle on T1-weighted images and variable low to high signal intensity on T2-weighted images depending on the edema and granulation tissue (Fig. 8.21). After repetitive attacks, subchondral erosions and small subchondral cysts may be seen reflecting intraosseous deposits of tophi [38]. The most specific imaging modality for urate deposition is dual-energy CT which can confirm or rule out gout disease with near 100 % accuracy [39].

Calcium Pyrophosphate Dihydrate Crystal Deposition (CPPD) or Pseudogout

Calcium pyrophosphate dihydrate crystal deposition is the result of crystal deposition in the synovium, the cartilage, the menisci, the periarticular tissue, and the intervertebral disk. It can be idiopathic or may be associated with other metabolic disorders, including hyperparathyroidism, gout, hypomagnesemia, Wilson's disease, acromegaly, hemochromatosis, and hypophosphatasia [40]. The acute form commonly affects the knee, and MR imaging reveals thickening of the synovium with calcium deposits, joint effusion, and calcified low-signal-intensity loose bodies. In the chronic form, MR imaging shows an accelerated form of a destructive arthritis. Cartilage and meniscal calcifications are better seen on gradi-

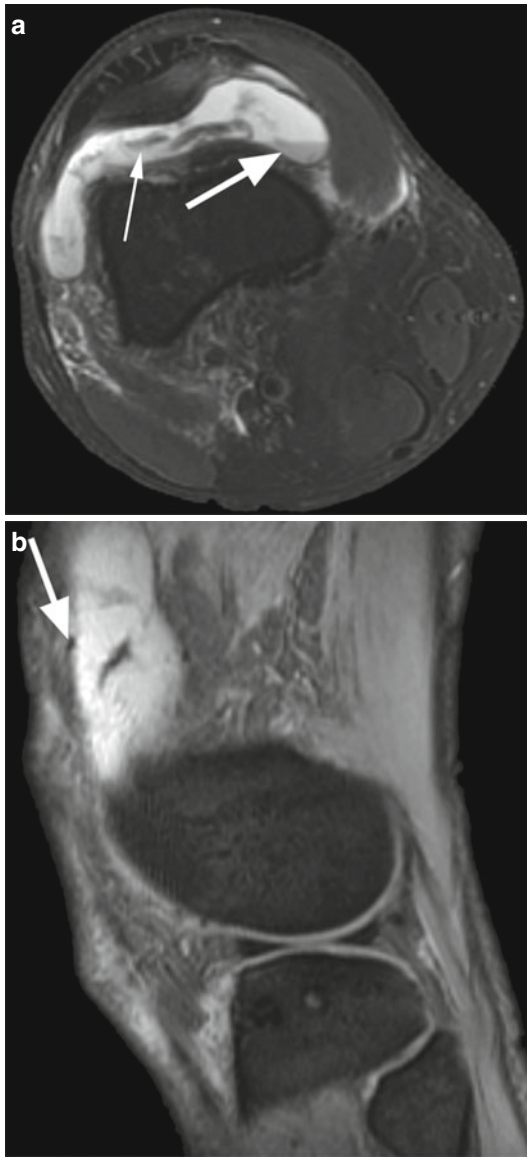

Fig. 8.27 Hemosiderotic synovitis in a 29 year old hemophiliac male. Axial proton-density (PD) fat-suppressed image (**a**) shows hemarthrosis with double-layer appearance. The inferior level is represented by cellular debris of intermediate signal intensity (*large arrow*). The synovium is thickened owing to intrasynovial fibrous scarring (*small arrow*). Sagittal T2-weighted fat-suppressed image (**b**) demonstrates a small area of hemosiderin-laden synovium (*arrow*)

ent-echo sequences because of the blooming artifacts. Calcifications of low signal intensity on all MR sequences are commonly encountered in the periarticular soft tissue.

Basic Calcium Phosphate Crystal Deposition (Hydroxyapatite)

Hydroxyapatite deposition is the most common deposition disease and most frequently affects the shoulder. Crystal deposition may be identified on MR imaging due to intra-articular foreign bodies, calcified tendons insertions, cartilage destruction, and subchondral cysts and erosions. In some cases, deposition near the origin or insertion of tendons may simulate a malignant bone neoplasm [41].

Amyloidosis

Amyloid deposition involves the synovial membrane, which shows focal nodules or bulky masses [2]. Amyloid arthropathy has been well documented as a complication in long-term dialysis patients and usually occurs at least 5 years after treatment [12]. MR imaging identifies the nodules which have a signal intensity that is in between that of cartilage and muscle. Subchondral cysts and small erosions are also often present.

8.2.4 Bursitis

Bursitis may be acute or chronic and may be caused by local or systemic processes such as trauma, overuse, infection, inflammatory arthropathy, and tumors. Thickening of the synovial membrane and effusion make the bursa visible on MR images as fluid collections with low signal on T1-weighted images and high signal on T2-weighted images in acute cases. In chronic cases, the inflamed bursa appears as an inhomogeneous mass mainly due to thickening, calcifications, and hemorrhage [3]. Diffuse inflammation of the soft tissue in the vicinity of bursitis may be present. Most of the bursae around the knee are only visible in pathological conditions, and the clinical symptoms and the etiology may differ between different bursae (Table 8.4). However, to establish a correct diagnosis is important for the differentiation from other intra- or extra-articular disorders and for avoiding unneces-

Table 8.4 Etiology and clinical manifestations of bursitis [3, 42–49]

	Etiology of bursitis	Clinical symptoms
Suprapatellar bursitis (Fig. 8.28)	Synovitis, infections, trauma, inflammatory and degenerative joint disorders, tumors; isolated bursitis is uncommon	Anterior knee pain; soft tissue mass may be palpated
Prepatellar bursitis (Fig. 8.29)	Overuse injury or trauma; occupational kneeling or crawling (housemaid's knee, carpet layer's knee)	Focal pain and swelling anterior to patella
Superficial infrapatellar or pretibial bursitis (Fig. 8.30)	Trauma or occupational overuse (clergyman's knee)	Pain anterior to tibial tubercle
Deep infrapatellar bursitis (Fig. 8.29)	Extensor mechanism overuse; runners and jumpers	Anterior knee pain; may mimic patellar tendinitis
Gastrocnemius-semimembranosus bursa	*See* Baker's cyst	*See* Baker's cyst
Iliotibial bursitis	Overuse injury in runners	Anterolateral knee pain; may mimic iliotibial tendinitis
Lateral collateral ligament-biceps femoris bursitis	Trauma	Pain and swelling along the lateral side
Medial collateral bursitis (Fig. 8.25)	Genu valgum, trauma, osteoarthritis, osteophytic spurs, rheumatoid disorders, flatfoot deformity; horseback riding, motorcycling	Pain along the medial side over the medial collateral ligament; palpable nodule at the medial side of the knee
Pes anserinus bursitis (Fig. 8.31)	Rheumatoid arthritis or osteoarthritis especially in overweight middle-aged to elderly women; runners	Vague medial knee pain; tenderness and swelling along the proximal medial tibia; may mimic meniscal or medial collateral ligament injury
Medial collateral ligament-semimembranosus bursitis	Repetitive or acute trauma; valgus stress	Focal pain along the posteromedial knee at the level of knee joint

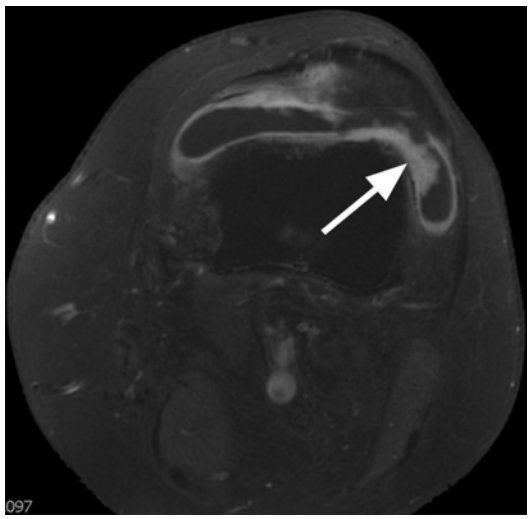

Fig. 8.28 Acute suprapatellar bursitis in a 46 year old patient with knee arthritis. Axial T1-weighted fat-suppressed postcontrast image shows irregular thickening and increased enhancement of the synovial membrane (*arrow*)

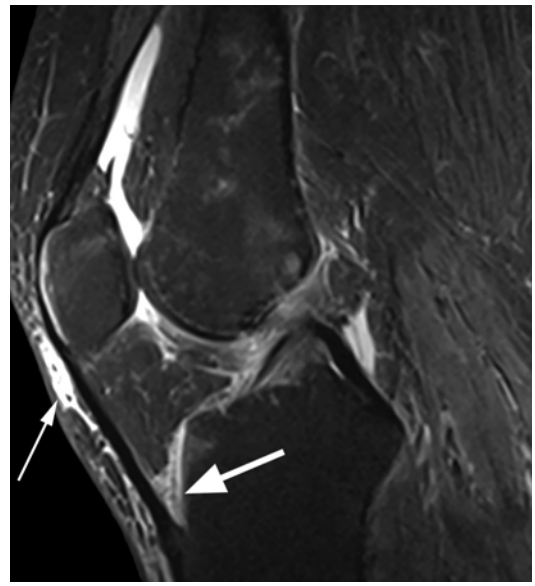

Fig. 8.29 Prepatellar bursitis and deep infrapatellar bursitis in a 56 year old male. Sagittal T2-weighted fat-suppressed image shows inflammation of the deep infrapatellar bursa (*large arrow*) and fluid collection in the prepatellar bursa (*small arrow*)

Fig. 8.30 Superficial pretibial bursitis in a 36 year old female. Sagittal T2-weighted fat-suppressed image shows fluid collection anterior to the tibial tubercle (*arrow*)

sary arthroscopy. Within the fluid accumulation of the bursae, loose bodies may be identified. Predominant locations are the suprapatellar bursa and the gastrocnemius-semimembranosus bursa.

Adventitial Bursitis

In contrast to the inherent anatomic bursae, there are also bursae which develop secondarily as a result of the increased friction between a normal tendon, muscle, or ligament and a pathologic point such as osteochondroma. Adventitial bursitis may appear also between orthopedic hardware and normal anatomical knee structures.

8.2.5 Synovial Cysts

Synovial cysts are juxta-articular fluid collections lined by synovial cells that may or may not communicate with the joint and may extend in any direction [44, 50]. The presence of the synovial lining allows the distinction from other cystic lesion, and its presence makes the disorders that affect the knee synovium affect the synovial cysts as well (inflammatory synovitis, metabolic synovitis, hemorrhage, synovial osteochondromatosis). Synovial cysts are often discovered incidentally in routine MRI examinations. The most specific type of synovial cyst is the popliteal (Baker's) cyst.

Popliteal (Baker's) Cyst

The term popliteal cyst refers to the fluid collection in the gastrocnemius-semimembranosus bursa. The cyst communicates with the knee joint and with the medial gastrocnemius bursa. The incidence of popliteal cyst on MRI reported in the literature ranges from 5 to 38 % and is significantly higher in patients over 50 years [51–54]. There is a high association between joint effusion and osteoarthritis and the popliteal cyst. Several internal derangements of the knee coexist with popliteal cyst even in the absence of joint effusion [52]. Tears of the posterior horn of the medial meniscus, lateral meniscal tears, bilateral meniscal tears, and anterior cruciate ligament tears are associated with popliteal cyst [3]. Patients may be asymptomatic or may complain with palpable mass in the popliteal fossa, posterior knee pain, calf claudication due to compression of the popliteal artery, or symptoms of nerve compression [54, 55]. On MR imaging, uncomplicated simple popliteal cyst appears as lobulated multilocular hypointense on T1-weighted images and hyperintense on T2-weighted images fluid mass between semimembranosus and gastrocnemius tendons that may extend over a variable distance superiorly or inferiorly (Fig. 8.32). In the case of complicated popliteal cyst, the MR imaging appearance is inhomogeneous demonstrating foci of hemorrhage and calcifications. Rupture of the cyst is identified as diffuse fluid of high signal T2-weighted intensity in the surrounding muscles and in the subcutaneous tissue (Fig. 8.33).

8.2.6 Ganglion Cysts

Ganglion cysts are tumor-like lesions surrounded by a dense capsule of connective tissue and are found in locations that are under constant stress. They are filled with mucoid material because of mucoid cystic degeneration in collagenous structures [56]. The ganglia are classified into intra-

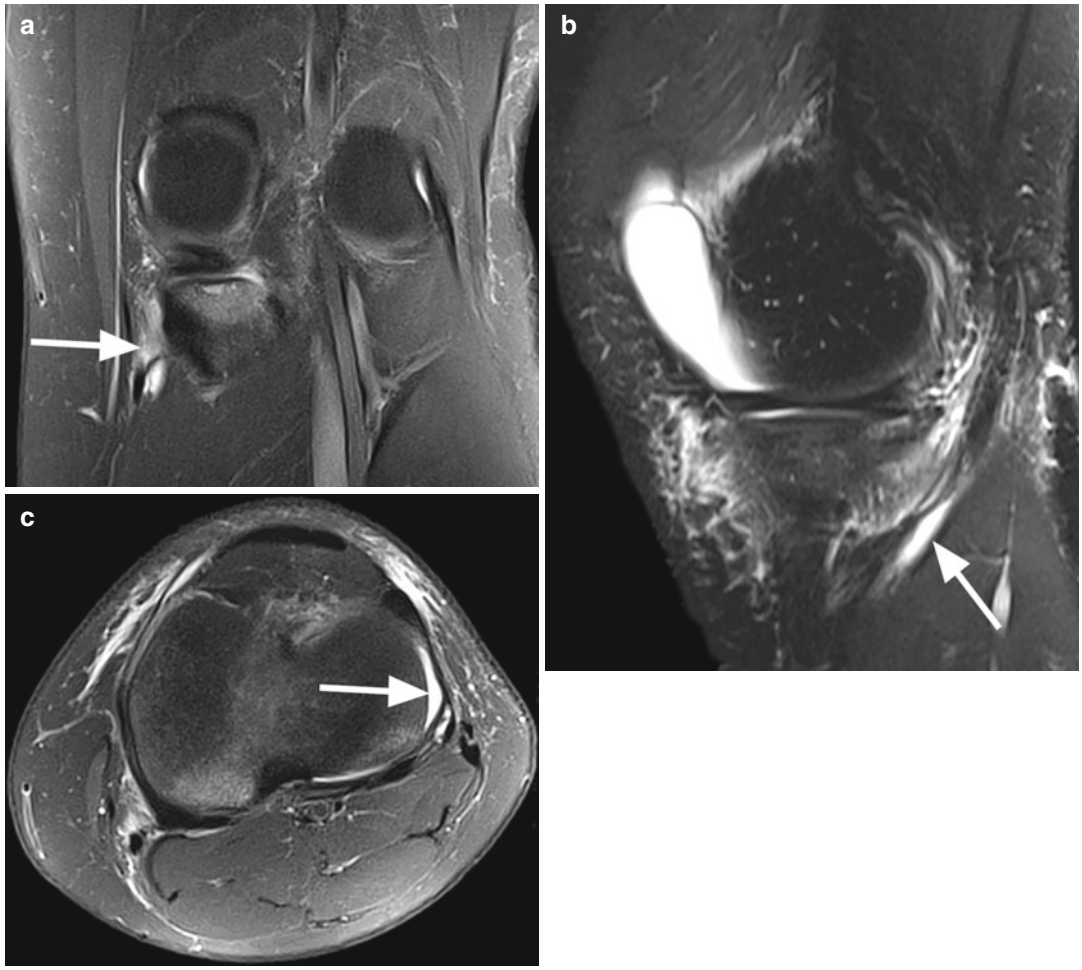

Fig. 8.31 Pes anserinus bursitis in a 47 year old female. Coronal proton-density (PD) fat-suppressed image (**a**), sagittal T2-weighted fat-suppressed image (**b**), and axial proton-density (PD) fat-suppressed image (**c**) show fluid collection in the pes anserinus bursa (*arrows*)

articular, extra-articular, and periosteal ganglia [3]. On MR imaging, they all appear as well-delineated rounded mass of hypointensity or intermediate signal intensity on T1-weighted images, of high signal intensity on T2-weighted images (compared to skeletal muscle), and with peripheral enhancement on postcontrast fat-suppressed T1-weighted images.

Intra-articular Ganglion Cysts

Intra-articular ganglion cysts are an uncommon finding (Fig. 8.34). A prevalence of 0.2–1.9 % on knee imaging or arthroscopy is reported [57–61]. They are extrasynovial and intracapsular and rarely communicate with the joint. Usually, they are associated with the cruciate ligaments, the infrapatellar fat pad, and the posterior capsule. No association was described with cruciate ligament tears. The clinical symptoms are pain, tenderness, limitation of motion, clicking, and palpable mass depending on the location [58–61]. Mucoid degeneration of the ligaments and ganglion cysts likely represents manifestations of the same pathology (Fig. 8.35) [62]. The ganglion cysts associated with the anterior cruciate ligament are fusiform and tend to extend along the ligament, whereas the cysts associated with posterior cruciate ligament or the infrapatellar fat

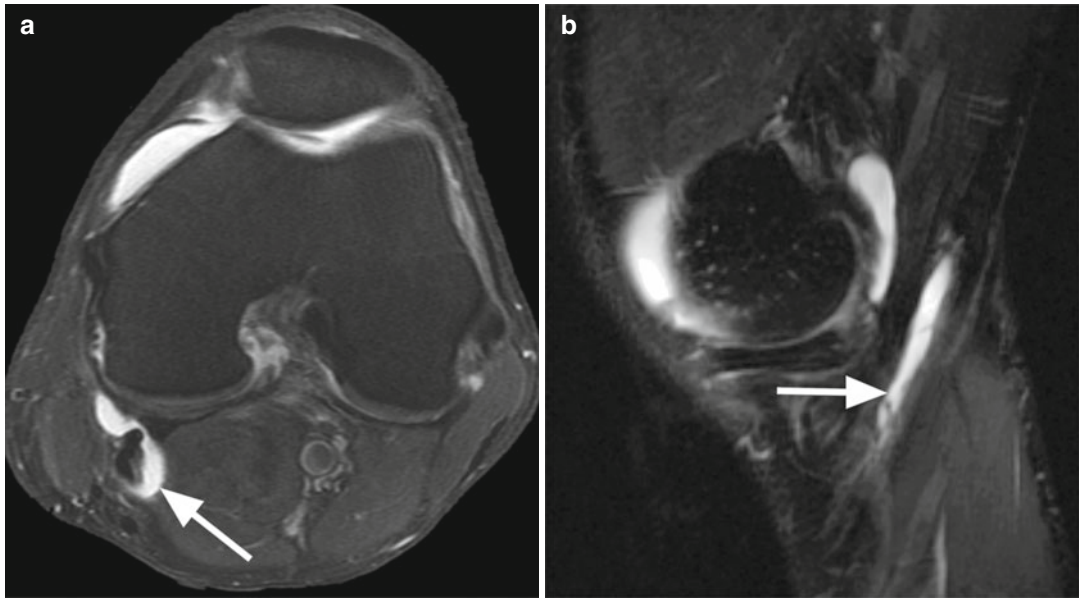

Fig. 8.32 Uncomplicated popliteal or Baker's cyst in a 49 year old male. Axial proton-density (PD) fat-suppressed image (**a**) and sagittal T2-weighted fat-suppressed image (**b**) show the fluid collection in the gastrocnemius-semimembranosus bursa (*arrows*). Baker's cyst may extend superior or inferior along the semimembranosus and gastrocnemius tendons

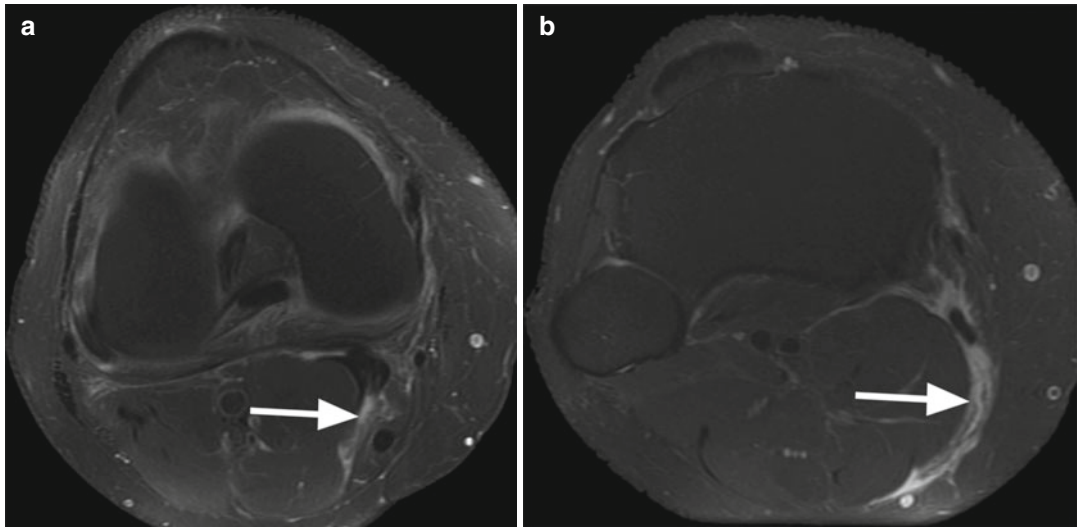

Fig. 8.33 Complicated popliteal or Baker's cyst in a 53 year old male. Two axial proton-density (PD) fat-suppressed images (**a**, **b**) show diffuse collection which extends distally along the medial gastrocnemius muscle (*arrows*) suggestive for rupture of the Baker's cyst

pad are more often multiloculated (Fig. 8.36) [63]. Ganglion cysts within the infrapatellar fat pad are most often located anterior to the anterior horn of the lateral meniscus.

Intraosseous ganglion cysts are located in the epiphyses of the bones and are associated with mucoid degeneration and ganglion cyst of cruciate ligaments [62]. They are

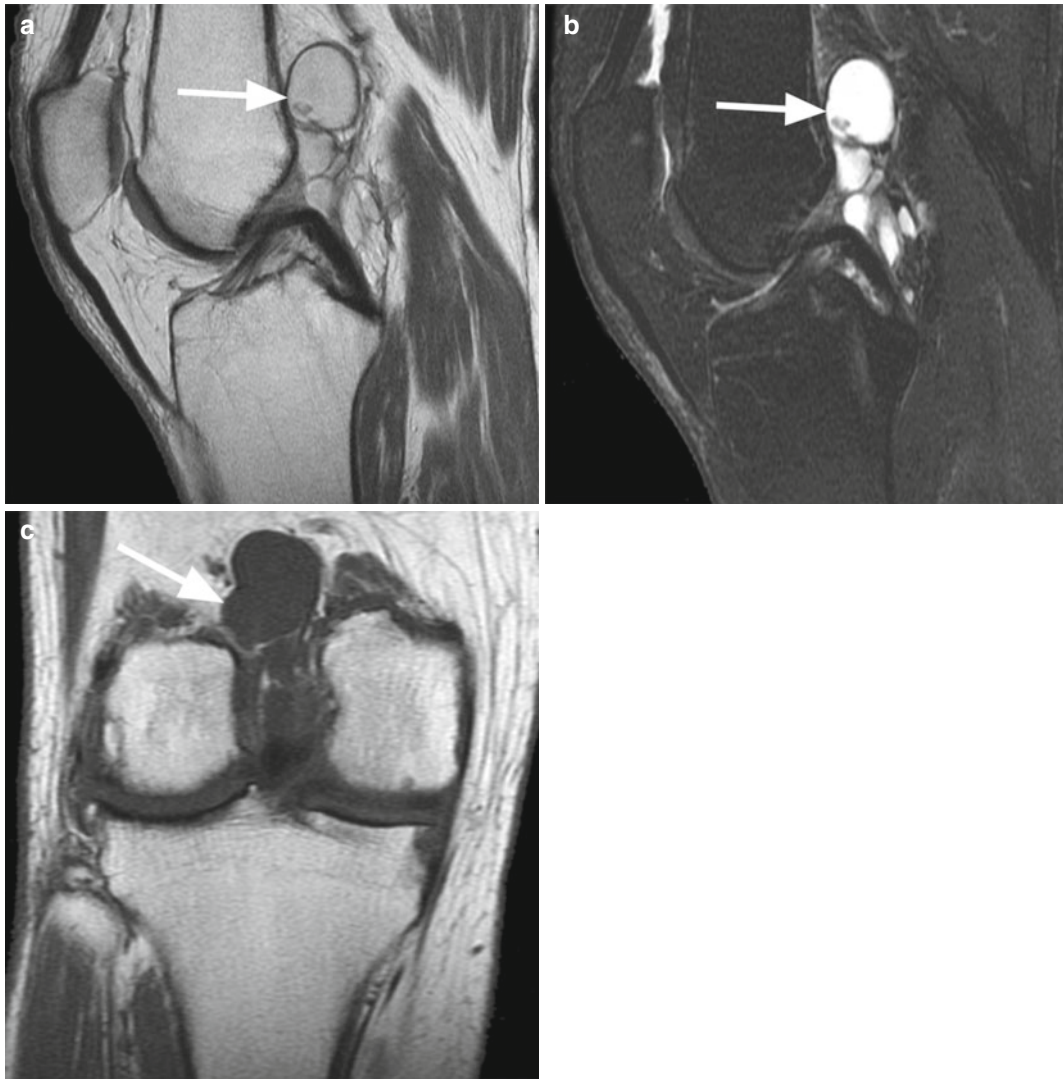

Fig. 8.34 Popliteal ganglion cyst in 71 year old female. Sagittal proton-density (PD)image (**a**), sagittal T2-weighted fat-suppressed image (**b**) and coronal T1-weighted image (**c**) show an intraarticular lobulated and septate cystic mass located in the popliteal fossa (*arrows*)

well-delineated unilocular or multilocular (Fig. 8.37).

Extra-articular Ganglion Cyst

Extra-articular ganglion cysts may arise from joint capsule, tendon sheath, ligaments, muscles, or bursae. Although they rarely communicate with the joint, the detection of a possible communication is important in planning the surgery [44]. Bone erosions and dissection along the tissue planes may occur [44, 57].

Periosteal Ganglion Cyst

Periosteal ganglion cysts are very rare, occur more frequently in men, and are the result of mucoid degeneration of the periosteum [3]. They produce erosions and reactive periosteal reaction with symptoms such as pain and swelling

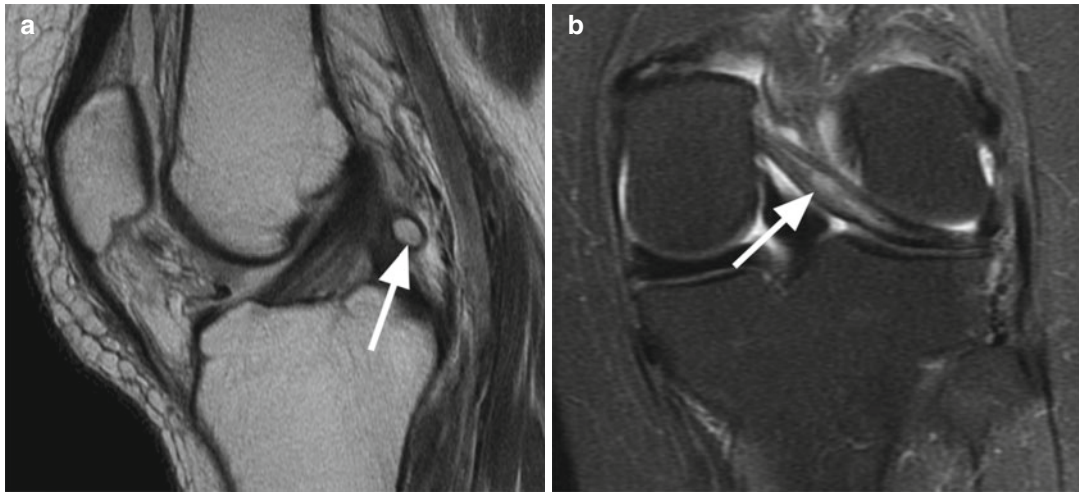

Fig. 8.35 Mucoid degeneration of the Wrisberg ligament in a 43 year old male. Sagittal proton-density (PD) image (**a**) and coronal proton-density (PD) fat-suppressed image (**b**) show a ganglion cyst of the Wrisberg ligament (*arrows*) resulting from mucoid degeneration of the ligament

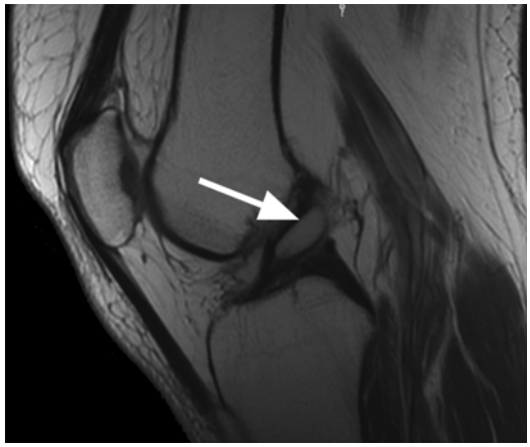

Fig. 8.36 Ganglion cyst of the anterior cruciate ligament (ACL) in a 53 year old female. Sagittal proton-density (PD) image shows a fusiform ganglion cyst of the anterior cruciate ligament (*arrow*)

[64, 65]. The most common location is in close proximity of the pes anserinus, in the proximal tibial shaft [64, 65].

8.2.7 Synovial Plica Syndrome

Plica syndrome is defined as a painful impairment of knee function in which the only finding is the presence of thickened plica [4]. The plica syndrome is a rather obscured and unappreciated pathological entity [66]. Trauma, a sudden increase in athletic activity, synovial foreign bodies, or any form of synovitis may lead to inflammation of synovial plica. The result is fibrosis and thickening of the synovial fold that may impinge against intra-articular structures, often creating localized cartilage pathology of the femoropatellar joint [66]. These result in pain, snapping, or pseudolocking during knee flexion. The infrapatellar and the mediopatellar plica syndromes are the most common. A symptomatic plica may be palpable especially when the hypertrophied plica resembles a soft tissue mass [67, 68]. Because of the anterior pain, especially in the mediopatellar plica syndrome, the symptoms may mimic the clinical findings of a medial

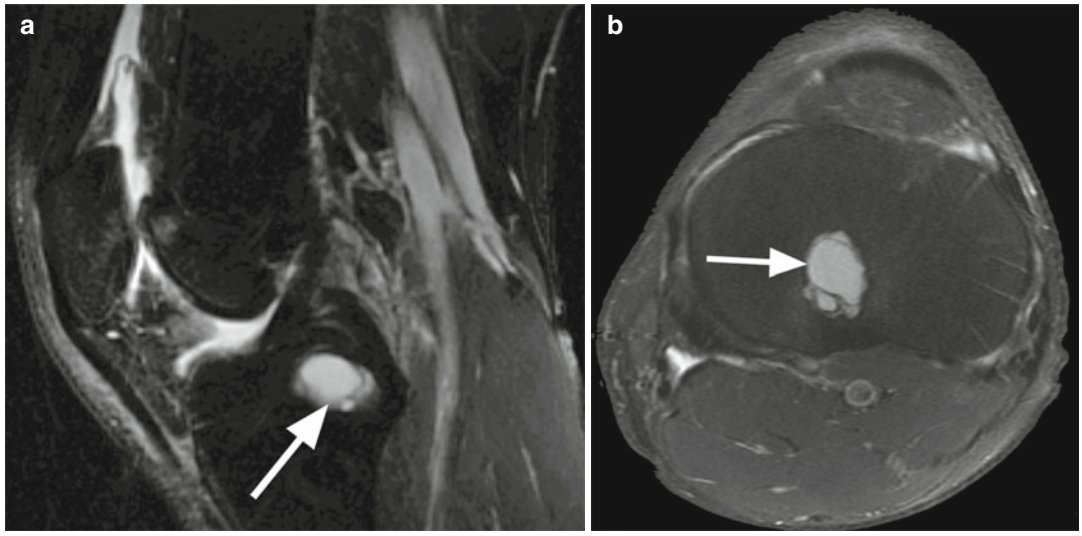

Fig. 8.37 Intraosseous ganglion cysts in a 49 year old male. Sagittal T2-weighted fat-suppressed image (**a**) and axial proton-density (PD) fat-suppressed image (**b**) show an intraosseous cystic lesion of the proximal tibial epiphysis (*arrows*)

meniscus tear [4]. Pathological plica appears on MR images as a thickened low-signal band or a small mass and is easily identified especially when joint fluid is present (Fig. 8.13). In chronic cases, cartilage damages or erosions may be seen in the femoropatellar joint. For any form of plica syndrome, a conservative treatment should be considered as the first choice especially in young patients.

Table 8.5 Classification of synovial tumor-like lesions and synovial tumors

Benign	Malignant
Synovial osteochondromatosis	Synovial sarcoma
Pigmented villonodular synovitis (PVNS)	Synovial chondrosarcoma
Localized nodular synovitis	Metastases
Lipoma arborescens	
Synovial hemangioma	

8.2.8 Synovial Tumor-Like Lesions and Synovial Tumors (Table 8.5)

Synovial Osteochondromatosis

Primary synovial osteochondromatosis is an uncommon benign synovial disorder characterized by formation of round metaplastic cartilaginous subsynovial nodules or osseous loose bodies in joints, tendon sheaths, or bursae. The nodules may contain calcifications, cartilage and bone, or only cartilage (synovial chondromatosis) [69–71]. There is no association between synovial osteochondromatosis and previous trauma, and the knee is the most affected joint. Clinically it manifests with pain, swelling, and limitation of motion [72]. Osteochondromatosis appears on MR imaging as soft tissue mass with internal nodules variable in size (from 2.0 mm to 1.0 cm). The presence of joint effusion is a typical sign in all forms of osteochondromatosis. The nodular lesions that are exclusively cartilaginous are hypointense or isointense to the muscle on T1-weighted images and of high signal on T2-weighted images. Uncalcified lesions are sometimes difficult to distinguish from the joint effusion on unenhanced images, but on postcontrast fat-suppressed T1-weighted MR images, the nodules show enhancement and are easy to differentiate from the synovial fluid. The presence of calcifications or bone within the nodules leads to an inhomogeneous MRI appearance

with low-signal-intensity foci (calcifications) or high-signal-intensity lesion on T1-weighted images showing signal suppression on fat-saturated images (fatty marrow in bony lesions) (Fig. 8.38) [73]. Subchondral erosions may also be seen but typically in more aggressive forms of the disease. Intra-articular cartilaginous or osseous loose bodies with joint effusion and hypertrophy of synovial membrane may be seen in idiopathic epiphyseal osteonecrosis, osteochondral fracture, and osteochondritis dissecans. This particular condition is referred by some authors as *secondary synovial osteochondromatosis with loose bodies* [74].

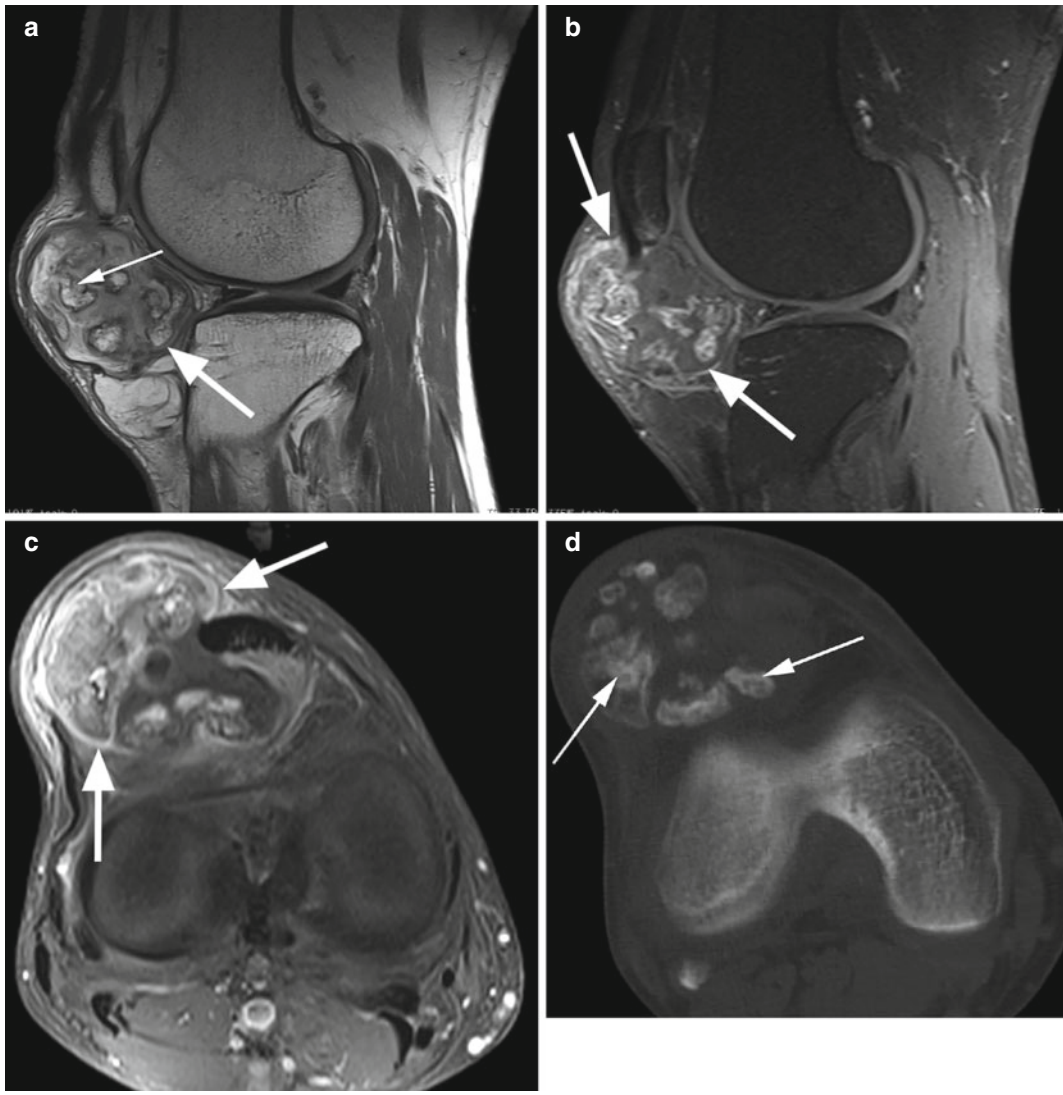

Fig. 8.38 Primary synovial osteochondrosarcoma in a 55 year old male. Sagittal proton-density (PD) image (**a**) shows an intraarticular well delineated mass (*large arrow*) in the infrapatellar fat pad. The lesion is highly inhomogeneous with a large amount of calcified cartilage (*small arrow*). After contrast administration, sagittal (**b**) and axial (**c**) T1-weighted fat-supressed images show inhomogeneous enhancement (*arrows* in **a** and **b**). CT image (**d**) demonstrates the calcified cartilage within the tumor (*arrows* in **g**). A definite differential diagnosis between osteochondrosarcoma and osteochondroma is practically imposible based only on the imaging findings

Pigmented Villonodular Synovitis (PVNS)

Pigmented villonodular synovitis is a benign slow-growing proliferative disorder that produces localized or diffuse nodular thickening of the synovial membrane. The disease is locally invasive, and the localized intra-articular form occurs almost exclusively in the knee [26]. The diffuse intra-articular form usually affects the large joint, most commonly the knee and hip [26]. Hemosiderin deposition is common in all forms of disease, but the extent of hemosiderin is much more prominent in diffuse intra-articular forms [75]. The disease may also occur extra-articularly in a bursa (pigmented villonodular bursitis) or tendon sheath (pigmented villonodular tenosynovitis) [75]. The disease affects males and females equally, and the age of presentation is between the second and fifth decade of life. The patients complain of acute episodes of pain and swelling and functional mechanical symptoms like locking and catching. In the focal or nodular form of PVNS, MR imaging may reveal low-signal-homogeneous-intensity solitary mass on T1-weighted images with moderate contrast enhancement. Small hyperintense T1-weighted of xanthomatous foci may be also present. On T2-weighted images, the nodules are inhomogeneous low signal intensity as a result of hemosiderin deposit (Fig. 8.39). In the diffuse form of the disease, MRI shows heterogeneous diffuse plaque-like thickening with villonodular appearance of intermediate to low signal intensity on T1-weighted images, low signal intensity on T2-weighted images, and hyperintense on T1-weighted postcontrast images. Associated large joint effusion is common, but the cartilage is preserved and subchondral erosions may be seen only in late phases. Although, the definitive diagnosis is made by biopsy, the MR imaging findings are virtually pathognomonic for pigmented villonodular synovitis [76].

Localized Nodular Synovitis (Synovial Giant Cell Tumor)

Localized nodular synovitis (synovial giant cell tumor) is a benign neoplasm characterized histologically by proliferating histiocytes bearing lipids and hemosiderin with a variable number of multinuclear giant cells [77]. The knee is the preferred synovial joint affected, and patients may complain with anterior knee pain, meniscal symptoms, and locking [77, 78]. MR imaging is the best diagnosis tool and shows a mass lesion of low or intermediate high signal intensity on T1-weighted images, intermediate or moderate high signal intensity on T2-weighted images, and moderate enhancement on postcontrast T1-weighted images (Fig. 8.40). On gradient-echo MR images, blooming artifacts may appear

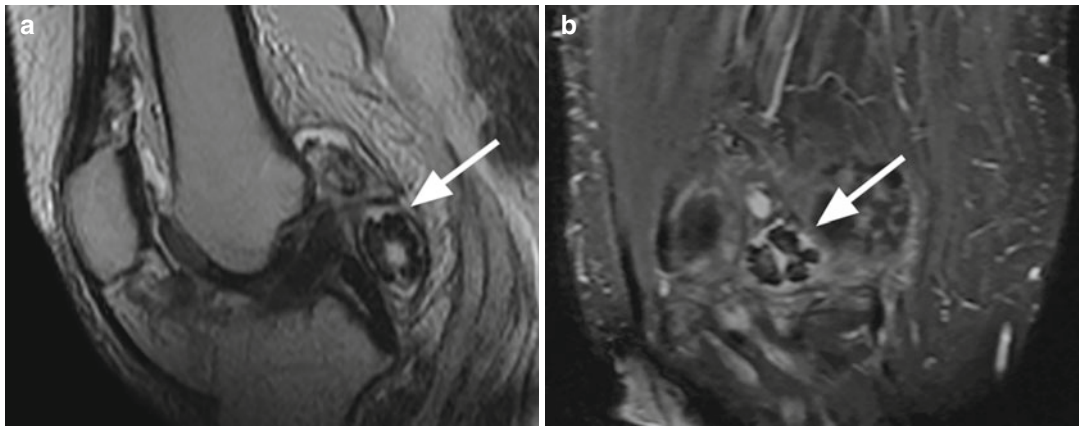

Fig. 8.39 Intra-articular pigmented villonodular synovitis in a 50 year old female. Sagittal proton-density (PD) image (**a**) and coronal proton-density (PD) fat-suppressed image (**b**) show a low-signal inhomogeneous solitary mass in the posterior synovial recess (*arrows*). Note the low signal intensity of hemosiderin deposition which is prominent in the intra-articular forms compared with the extra-articular forms

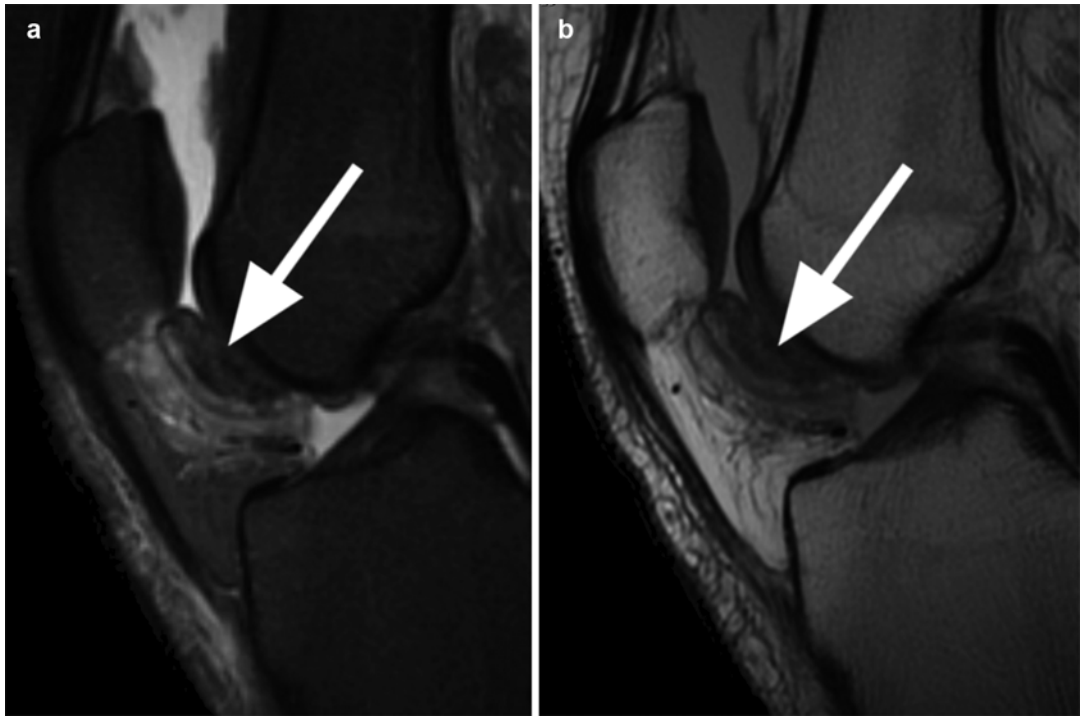

Fig. 8.40 Localized nodular synovitis (synovial giant cell tumor) in a 21 year old female. Sagittal T2-weighted fat-suppressed image (**a**) and sagittal proton-density (PD) image (**b**) show a mass lesion of low signal intensity located into the infrapatellar fat pad (*arrows*)

because of the presence of hemosiderin. The lesion is most commonly located within the infrapatellar fat pad and suprapatellar bursa.

Lipoma Arborescens (Villous Lipomatous Proliferation of the Synovial Membrane or Diffuse Synovial Lipoma)

Lipoma arborescens is one of the rarest benign synovial disorders and is characterized by fatty infiltration of the synovial membrane. It affects preferentially adult men [74]. The lesions can be multifocal and bilateral and can appear as high-signal-intensity fatty intra-articular mass on T1- and T2-weighted images (see Fig. 7.34). The synovial membrane is usually inflamed and enhances after contrast administration.

Synovial Hemangioma

Synovial hemangioma is vascular malformation that affects mainly children and young adults [79]. The lesion may be localized or diffuse and it manifests with pain and swelling. MR imaging may show an isointense T1-weighted to muscles lesion with dilated, tortuous vessels with signal flow void. The lesion enhances variably after contrast administration. Synovial hemangiomas may bleed and the MR imaging findings in these cases mimic hemosiderotic synovitis.

Synovial Sarcoma

Synovial sarcoma accounts for approximately 5 % of all soft tissue sarcomas with the vast majority representing secondary involvement by the tumor from immediate structures of the joint [80, 81]. One third of the cases occur in the lower extremity and are the most common soft tissue malignancy of the lower extremity in the 6- to 25-year age range [81]. The knee joint is the most common involved joint (88 %) [82]. There is a lack of specific findings on MR imaging that makes this entity to be considered in the differential diagnosis if imaging findings are not specific for another entity [82]. Usually, the tumor appears

as a cystic inhomogeneous well-delineated lobulated and septated mass with peripheral and septal enhancement [83, 84]. The tumor is in the proximity of the joint or within the joint and may be in contiguity with the bone or invading the bone [85]. Other MR imaging findings include calcifications, foci of hemorrhage, fluid-fluid levels, and the triple signal intensity appearance [85]. Calcifications are usually seen on radiographs and are present in up to 32 % of the cases [86]. The triple signal intensity appearance is seen on T2-weighted images and is defined by the presence of hyperintense, isointense, and hypointense lesions relative to the fat signal intensity translating the mixture of solid, cystic, fibrous, and hemorrhagic content [85].

Synovial Chondrosarcoma

Synovial chondrosarcoma is extremely rare and is not clear whether arises de novo or from malignant degeneration of synovial osteochondromatosis [79]. The MRI appearance is similar to synovial osteochondromatosis, and, therefore, there are no reliable distinguishing MRI findings between the two entities (Fig. 8.38). Distant metastases usually appear in the lung [87].

Synovial Metastases

Lung cancer is the most common cancer that metastasizes in the joints, and the knee joint is most frequently affected [88]. The result is a metastatic arthritis that can involve all structures of the knee joint: the synovium, cartilage, and bone. The diagnosis is made with biopsy or cytology of the joint effusion [79, 88].

8.3 MRI Impression

1. Joint effusion (within suprapatellar bursa, within recesses, within popliteal tendon sheath)
2. Hemarthrosis
3. Lipohemarthrosis (usually indicator of bone fracture)
4. Intra-articular bodies (specify the origin of the bodies):
   - Cartilage
   - Bone
   - Osteochondral fragment
   - Small nodules (in inflammatory synovitis)
   - Tophi in gout
   - Small hyaline cartilage (primary synovial osteochondromatosis)
   - Scattered nodules with “blooming” artifacts (pigmented villonodular synovitis or hemophilic arthropathy)
   - Metallic foreign bodies (correlation with clinical history)
   - Intra-articular gas
5. Synovitis (thickness >2–3 mm)
   - Inflammatory (associated bone marrow edema, erosions)
   - Osteoarthritis (associated cartilage loss, subchondral cysts)
   - Synovial thickening, bone marrow edema, erosions suggesting infectious synovitis
   - Hemosiderotic synovitis
   - Synovitis with crystal deposition (gout, calcium pyrophosphate dehydrate crystal deposition, hydroxyapatite)
   - Amyloid deposition
6. Bursitis (location of the involved bursa)
   - Complicated bursitis (loose bodies, calcifications, hemorrhage, soft tissue inflammation)
7. Adventitial bursitis – specify the cause of bursitis (osteochondroma, orthopedic hardware)
8. Synovial cyst (location)
   - Uncomplicated
   - Complicated (loose bodies, calcifications, hemorrhage, rupture, nerve or artery compression)
9. Ganglion cyst (intra-articular/extra-articular/periosteal)
10. Synovial plica thickening (suprapatellar, infrapatellar, mediopatellar, lateral patellar)
11. Synovial mass (correlated with clinical history)
    - Osteochondromatosis
    - Pigmented villonodular synovitis
    - Localized synovitis
    - Lipoma
    - Hemangioma
    - Sarcoma
    - Chondrosarcoma
    - Metastases

References

1. Steinberg PJ, Hodde KC. The morphology of synovial lining of various structures in several species as observed with scanning electron microscopy. Scanning Microsc. 1990;4(4):987–1019; discussion 1019–20.
2. Fenn S, Datir A, Saifuddin A. Synovial recesses of the knee: MR imaging review of anatomical and pathological features. Skeletal Radiol. 2009;38(4):317–28.
3. Beaman FD, Peterson JJ. MR imaging of cysts, ganglia, and bursae about the knee. Radiol Clin North Am. 2007;45(6):969–82, vi.
4. Garcia-Valtuille R, et al. Anatomy and MR imaging appearances of synovial plicae of the knee. Radiographics. 2002;22(4):775–84.
5. Doppman JL. Baker's cyst and the normal gastrocnemio-semimembranosus bursa. Am J Roentgenol Radium Ther Nucl Med. 1965;94:646–52.
6. Resnick D, et al. Proximal tibiofibular joint: anatomic-pathologic-radiographic correlation. AJR Am J Roentgenol. 1978;131(1):133–8.
7. Guerra Jr J, et al. Pictorial essay: gastrocnemio-semimembranosus bursal region of the knee. AJR Am J Roentgenol. 1981;136(3):593–6.
8. Johnson RL, De Smet AA. MR visualization of the popliteomeniscal fascicles. Skeletal Radiol. 1999; 28(10):561–6.
9. Munshi M, et al. MR imaging, MR arthrography, and specimen correlation of the posterolateral corner of the knee: an anatomic study. AJR Am J Roentgenol. 2003;180(4):1095–101.
10. Perdikakis E, Skiadas V. MRI characteristics of cysts and "cyst-like" lesions in and around the knee: what the radiologist needs to know. Insights Imaging. 2013;4(3):257–72.
11. Boles CA, Martin DF. Synovial plicae in the knee. AJR Am J Roentgenol. 2001;177(1):221–7.
12. Chung CB, Boucher R, Resnick D. MR imaging of synovial disorders of the knee. Semin Musculoskelet Radiol. 2009;13(4):303–25.
13. Schweitzer ME, et al. Knee effusion: normal distribution of fluid. AJR Am J Roentgenol. 1992;159(2): 361–3.
14. Hall FM. Radiographic diagnosis and accuracy in knee joint effusions. Radiology. 1975;115(1):49–54.
15. McCarthy D. Synovial fluid. In: McCarthy O, editor. Arthritis and allied conditions. 11th ed. Philadelphia: Lea & Febiger; 1989. p. 70–1.
16. Martin DJ, et al. Recurrent hemarthrosis associated with gout. Clin Orthop Relat Res. 1992;277:262–5.
17. Blyth T, et al. Subsynovial vascular abnormality causing recurrent hemarthrosis in an 84-year-old man. J Rheumatol. 1995;22(3):552–3.
18. Ryu KN, et al. Evolving stages of lipohemarthrosis of the knee. Sequential magnetic resonance imaging findings in cadavers with clinical correlation. Invest Radiol. 1997;32(1):7–11.
19. Gylys-Morin VM, et al. Knee in early juvenile rheumatoid arthritis: MR imaging findings. Radiology. 2001;220(3):696–706.
20. Hill CL, et al. Knee effusions, popliteal cysts, and synovial thickening: association with knee pain in osteoarthritis. J Rheumatol. 2001;28(6):1330–7.
21. Saddik D, McNally EG, Richardson M. MRI of Hoffa's fat pad. Skeletal Radiol. 2004;33(8):433–44.
22. Crema MD, et al. Peripatellar synovitis: comparison between non-contrast-enhanced and contrast-enhanced MRI and association with pain. The MOST study. Osteoarthritis Cartilage. 2013;21(3):413–8.
23. Sugimoto H, et al. Early-stage rheumatoid arthritis: diagnostic accuracy of MR imaging. Radiology. 1996;198(1):185–92.
24. Frick MA, Wenger DE, Adkins M. MR imaging of synovial disorders of the knee: an update. Radiol Clin North Am. 2007;45(6):1017–31, vii.
25. Narvaez JA, et al. MR imaging assessment of clinical problems in rheumatoid arthritis. Eur Radiol. 2002; 12(7):1819–28.
26. Jaganathan S, et al. Spectrum of synovial pathologies: a pictorial assay. Curr Probl Diagn Radiol. 2012; 41(1):30–42.
27. Huang TL, et al. Intra-articular rheumatoid nodule of the knee joint associated with recurrent subluxation of the patella. A case report. J Bone Joint Surg Am. 1979;61(3):438–40.
28. McGonagle D, Gibbon W, Emery P. Classification of inflammatory arthritis by enthesitis. Lancet. 1998;3 52(9134):1137–40.
29. Crema MD, et al. Magnetic resonance imaging assessment of subchondral bone and soft tissues in knee osteoarthritis. Rheum Dis Clin North Am. 2009;35(3): 557–77.
30. Roemer FW, et al. The association of meniscal damage with joint effusion in persons without radiographic osteoarthritis: the Framingham and MOST osteoarthritis studies. Osteoarthritis Cartilage. 2009;17(6):748–53.
31. Hill CL, et al. Synovitis detected on magnetic resonance imaging and its relation to pain and cartilage loss in knee osteoarthritis. Ann Rheum Dis. 2007; 66(12):1599–603.
32. Erdman WA, et al. Osteomyelitis: characteristics and pitfalls of diagnosis with MR imaging. Radiology. 1991;180(2):533–9.
33. Graif M, et al. The septic versus nonseptic inflamed joint: MRI characteristics. Skeletal Radiol. 1999;28(11): 616–20.
34. Stein H, Duthie RB. The pathogenesis of chronic haemophilic arthropathy. J Bone Joint Surg Br. 1981; 63B(4):601–9.
35. Luck JV Jr, Kasper CK. Surgical management of advanced hemophilic arthropathy. An overview of 20 years' experience. Clin Orthop Relat Res. 1989;(242): 60–82.http://www.ncbi.nlm.nih.gov/pubmed/2650951.
36. Rand T, et al. Magnetic resonance imaging in hemophilic children: value of gradient echo and contrast-enhanced imaging. Magn Reson Imaging. 1999;17(2): 199–205.
37. Devaney K, Vinh TN, Sweet DE. Synovial hemangioma: a report of 20 cases with differential diagnostic considerations. Hum Pathol. 1993;24(7):737–45.

38. Monu JU, Pope Jr TL. Gout: a clinical and radiologic review. Radiol Clin North Am. 2004;42(1):169–84.
39. Bongartz T, et al. Dual-energy CT for the diagnosis of gout: an accuracy and diagnosis yield study. Ann Rheum Dis doi:10.1136/annrheumdis-2013-205095
40. Ahn JK, et al. Idiopathic calcium pyrophosphate dihydrate (CPPD) crystal deposition disease in a young male patient: a case report. J Korean Med Sci. 2003;18(6):917–20.
41. Hayes CW, et al. Calcific tendinitis in unusual sites associated with cortical bone erosion. AJR Am J Roentgenol. 1987;149(5):967–70.
42. Stuttle FL. The no-name and no-fame bursa. Clin Orthop. 1959;15:197–9.
43. Kerlan RK, Glousman RE. Tibial collateral ligament bursitis. Am J Sports Med. 1988;16(4):344–6.
44. Janzen DL, et al. Cystic lesions around the knee joint: MR imaging findings. AJR Am J Roentgenol. 1994;163(1):155–61.
45. Forbes JR, Helms CA, Janzen DL. Acute pes anserine bursitis: MR imaging. Radiology. 1995;194(2):525–7.
46. Rothstein CP, et al. Semimembranosus-tibial collateral ligament bursitis: MR imaging findings. AJR Am J Roentgenol. 1996;166(4):875–7.
47. LaPrade RF, Hamilton CD. The fibular collateral ligament-biceps femoris bursa. An anatomic study. Am J Sports Med. 1997;25(4):439–43.
48. LaPrade RF. The anatomy of the deep infrapatellar bursa of the knee. Am J Sports Med. 1998;26(1):129–32.
49. De Maeseneer M, et al. MR imaging of the medial collateral ligament bursa: findings in patients and anatomic data derived from cadavers. AJR Am J Roentgenol. 2001;177(4):911–7.
50. Steiner E, et al. Ganglia and cysts around joints. Radiol Clin North Am. 1996;34(2):395–425, xi–xii.
51. Fielding JR, Franklin PD, Kustan J. Popliteal cysts: a reassessment using magnetic resonance imaging. Skeletal Radiol. 1991;20(6):433–5.
52. Miller TT, et al. MR imaging of Baker cysts: association with internal derangement, effusion, and degenerative arthropathy. Radiology. 1996;201(1):247–50.
53. Marti-Bonmati L, et al. MR imaging of Baker cysts – prevalence and relation to internal derangements of the knee. MAGMA. 2000;10(3):205–10.
54. Labropoulos N, Shifrin DA, Paxinos O. New insights into the development of popliteal cysts. Br J Surg. 2004;91(10):1313–8.
55. Robertson CM, Robertson RF, Strazerri JC. Proximal dissection of a popliteal cyst with sciatic nerve compression. Orthopedics. 2003;26(12):1231–2.
56. McCarthy CL, McNally EG. The MRI appearance of cystic lesions around the knee. Skeletal Radiol. 2004;33(4):187–209.
57. Burk Jr DL, et al. Meniscal and ganglion cysts of the knee: MR evaluation. AJR Am J Roentgenol. 1988; 150(2):331–6.
58. McLaren DB, Buckwalter KA, Vahey TN. The prevalence and significance of cyst-like changes at the cruciate ligament attachments in the knee. Skeletal Radiol. 1992;21(6):365–9.
59. Nokes SR, Koonce TW, Montanez J. Ganglion cysts of the cruciate ligaments of the knee: recognition on MR images and CT-guided aspiration. AJR Am J Roentgenol. 1994;162(6):1503.
60. Kang CN, et al. Intra-articular ganglion cysts of the knee. Arthroscopy. 1999;15(4):373–8.
61. Sumen Y, et al. Ganglion cysts of the cruciate ligaments detected by MRI. Int Orthop. 1999;23(1):58–60.
62. Bergin D, et al. Anterior cruciate ligament ganglia and mucoid degeneration: coexistence and clinical correlation. AJR Am J Roentgenol. 2004;182(5): 1283–7.
63. Kim MG, et al. Intra-articular ganglion cysts of the knee: clinical and MR imaging features. Eur Radiol. 2001;11(5):834–40.
64. McCarthy EF, et al. Periosteal ganglion: a cause of cortical bone erosion. Skeletal Radiol. 1983;10(4):243–6.
65. Abdelwahab IF, et al. Periosteal ganglia: CT and MR imaging features. Radiology. 1993;188(1):245–8.
66. Schindler OS. 'The Sneaky Plica' revisited: morphology, pathophysiology and treatment of synovial plicae of the knee. Knee Surg Sports Traumatol Arthrosc. 2014;22(2):247–62.
67. Apple JS, et al. Synovial plicae of the knee. Skeletal Radiol. 1982;7(4):251–4.
68. Trout TE, Bock H, Resnick D. Suprapatellar plicae of the knee presenting as a soft-tissue mass. Report of five patients. Clin Imaging. 1996;20(1):55–9.
69. Villacin AB, Brigham LN, Bullough PG. Primary and secondary synovial chondrometaplasia: histopathologic and clinicoradiologic differences. Hum Pathol. 1979;10(4):439–51.
70. Apte SS, Athanasou NA. An immunohistological study of cartilage and synovium in primary synovial chondromatosis. J Pathol. 1992;166(3):277–81.
71. Sviland L, Malcolm AJ. Synovial chondromatosis presenting as painless soft tissue mass–a report of 19 cases. Histopathology. 1995;27(3):275–9.
72. Milgram JW. Synovial osteochondromatosis: a histopathological study of thirty cases. J Bone Joint Surg Am. 1977;59(6):792–801.
73. McKenzie G, Raby N, Ritchie D. A pictorial review of primary synovial osteochondromatosis. Eur Radiol. 2008;18(11):2662–9.
74. O'Connell JX. Pathology of the synovium. Am J Clin Pathol. 2000;114(5):773–84.
75. Murphey MD, et al. Pigmented villonodular synovitis: radiologic-pathologic correlation. Radiographics. 2008;28(5):1493–518.
76. Hughes TH, et al. Pigmented villonodular synovitis: MRI characteristics. Skeletal Radiol. 1995;24(1): 7–12.
77. Nau T, et al. Giant-cell tumor of the synovial membrane: localized nodular synovitis in the knee joint. Arthroscopy. 2000;16(8):E22.
78. Yoo JH, Yang BK, Park JM. Localized nodular synovitis of the knee presenting as anterior knee pain: a case report. Knee. 2007;14(5):398–401.
79. Sheldon PJ, Forrester DM, Learch TJ. Imaging of intraarticular masses. Radiographics. 2005;25(1):105–19.

80. McKinney CD, Mills SE, Fechner RE. Intraarticular synovial sarcoma. Am J Surg Pathol. 1992;16(10): 1017–20.
81. Kransdorf MJ. Malignant soft-tissue tumors in a large referral population: distribution of diagnoses by age, sex, and location. AJR Am J Roentgenol. 1995;164(1): 129–34.
82. Bui-Mansfield LT, O'Brien SD. Magnetic resonance appearance of intra-articular synovial sarcoma: case reports and review of the literature. J Comput Assist Tomogr. 2008;32(4):640–4.
83. Ayoub KS, et al. Synovial sarcoma arising in association with a popliteal cyst. Skeletal Radiol. 2000;29(12): 713–6.
84. Namba Y, et al. Intraarticular synovial sarcoma confirmed by SYT-SSX fusion transcript. Clin Orthop Relat Res. 2002;395:221–6.
85. Jones BC, Sundaram M, Kransdorf MJ. Synovial sarcoma: MR imaging findings in 34 patients. AJR Am J Roentgenol. 1993;161(4):827–30.
86. Cadman NL, Soule EH, Kelly PJ. Synovial sarcoma; an analysis of 34 tumors. Cancer. 1965;18:613–27.
87. Taconis WK, van der Heul RO, Taminiau AM.Synovial chondrosarcoma: report of a case and review of the literature. Skeletal Radiol. 1997;26(11):682–5.
88. Thompson KS, et al. Synovial metastasis: diagnosis by fine-needle aspiration cytologic investigation. Diagn Cytopathol. 1996;15(4):334–7.